Ignition: Where Does it Happen?

$P = y g_{eff} = \text{const}$

Independent of latitude.

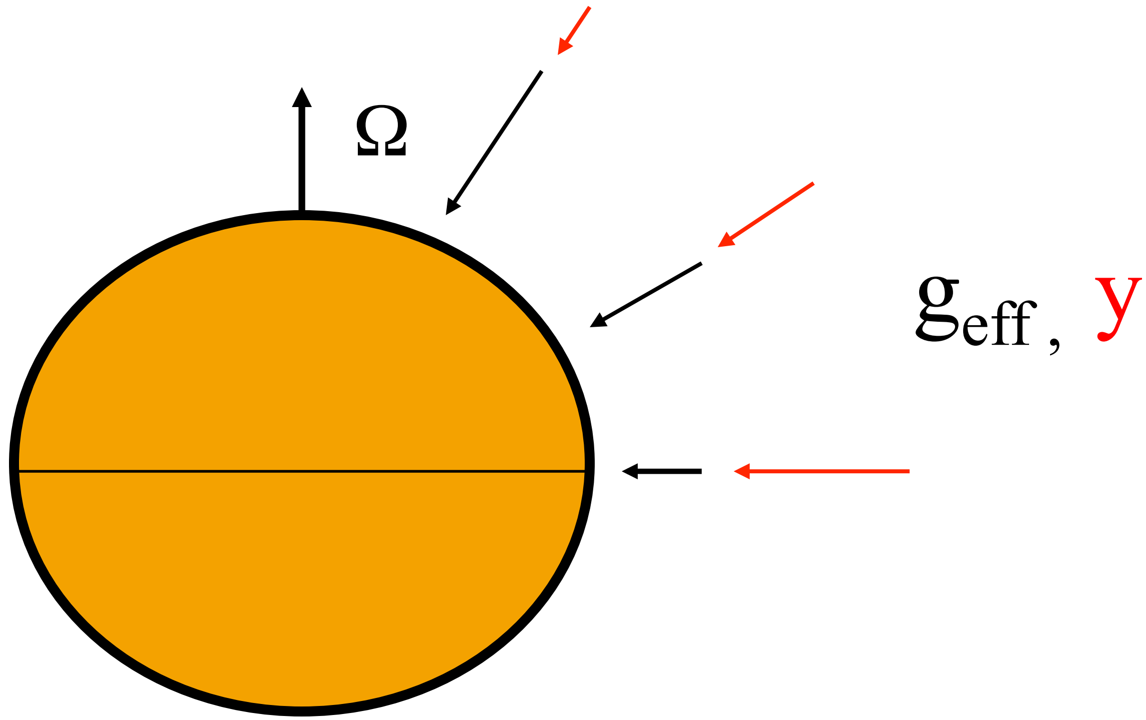

- Local accretion rate is higher at the equator. Preference for ignition near equator.
- Ignition stabilizes above a critical local accretion rate.
- At higher accretion rates, ignition could move off equator to higher latitudes (Cooper & Narayan 2007).
- Can we see this?

Rapid Spin and Ignition Latitude

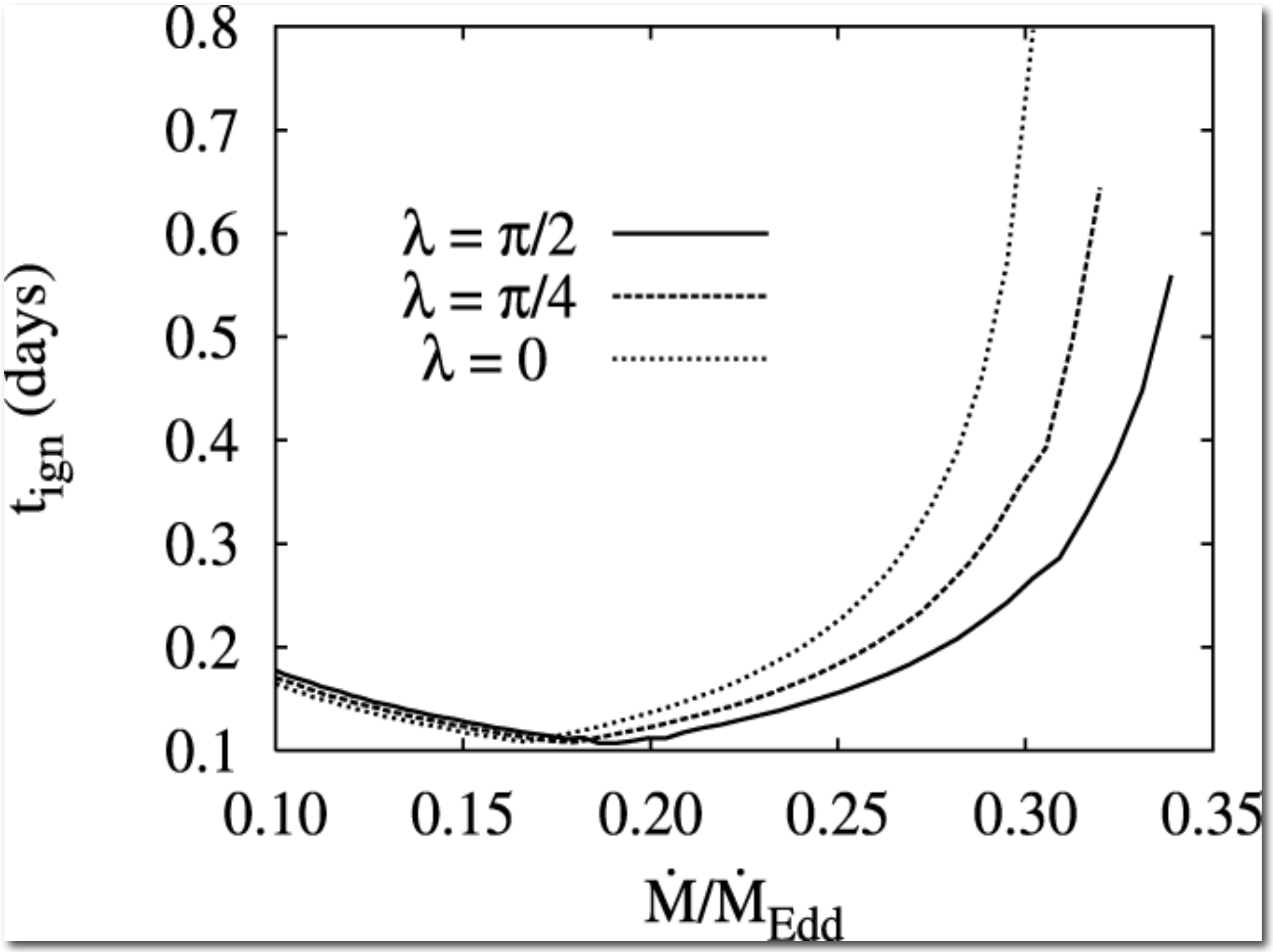

Cooper & Narayan (2007)

- Variation in effective gravity with latitude, give changes in ignition timescale with latitude.
- Higher accretion rates yield shorter ignition times away from equator.
- Need fast rotation.

Ignition, spreading, and the shape of the rising part of the light curve

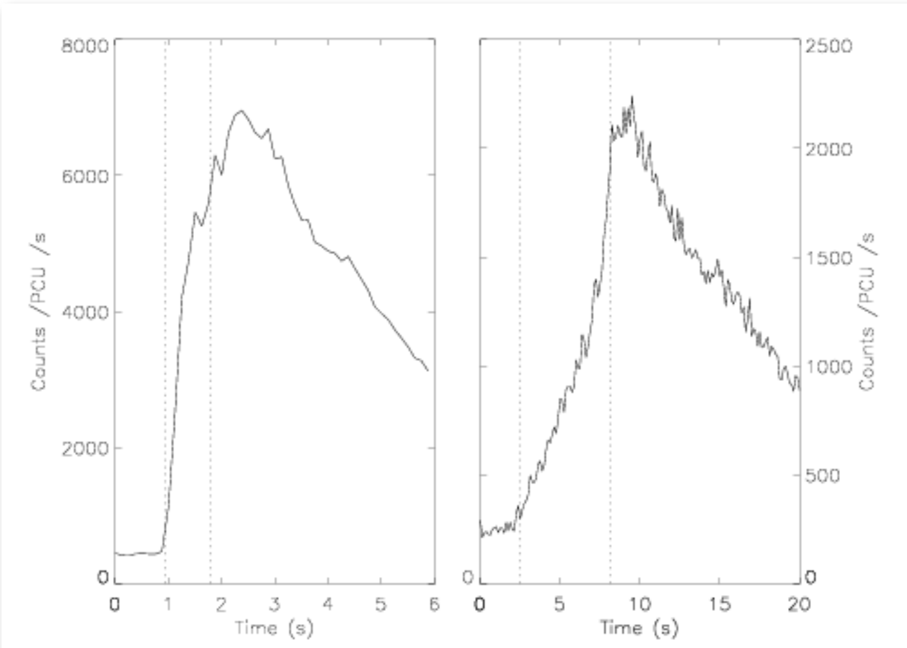

- Watts & Maurer (2007) explore shapes of burst rising phases.
- Find that bursts group according to peak flux and “convexity,” and suggest that ignition latitude varies with accretion rate.

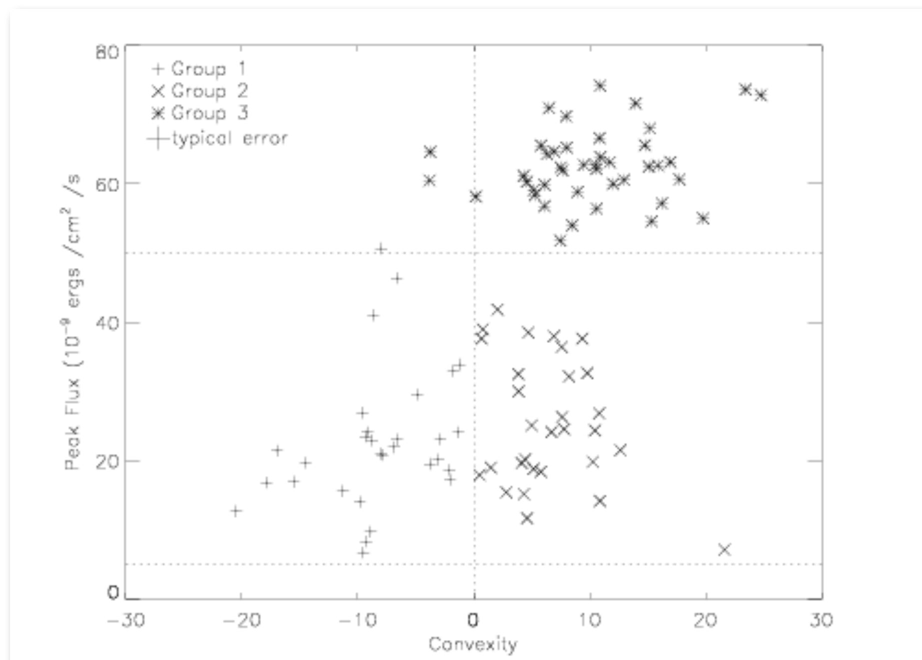

- Negative convexity bursts ignited at high latitude (near the pole).
- High flux, positive convexity bursts are He ignited near the equator

Puzzle: Oscillations in the Cooling Phase

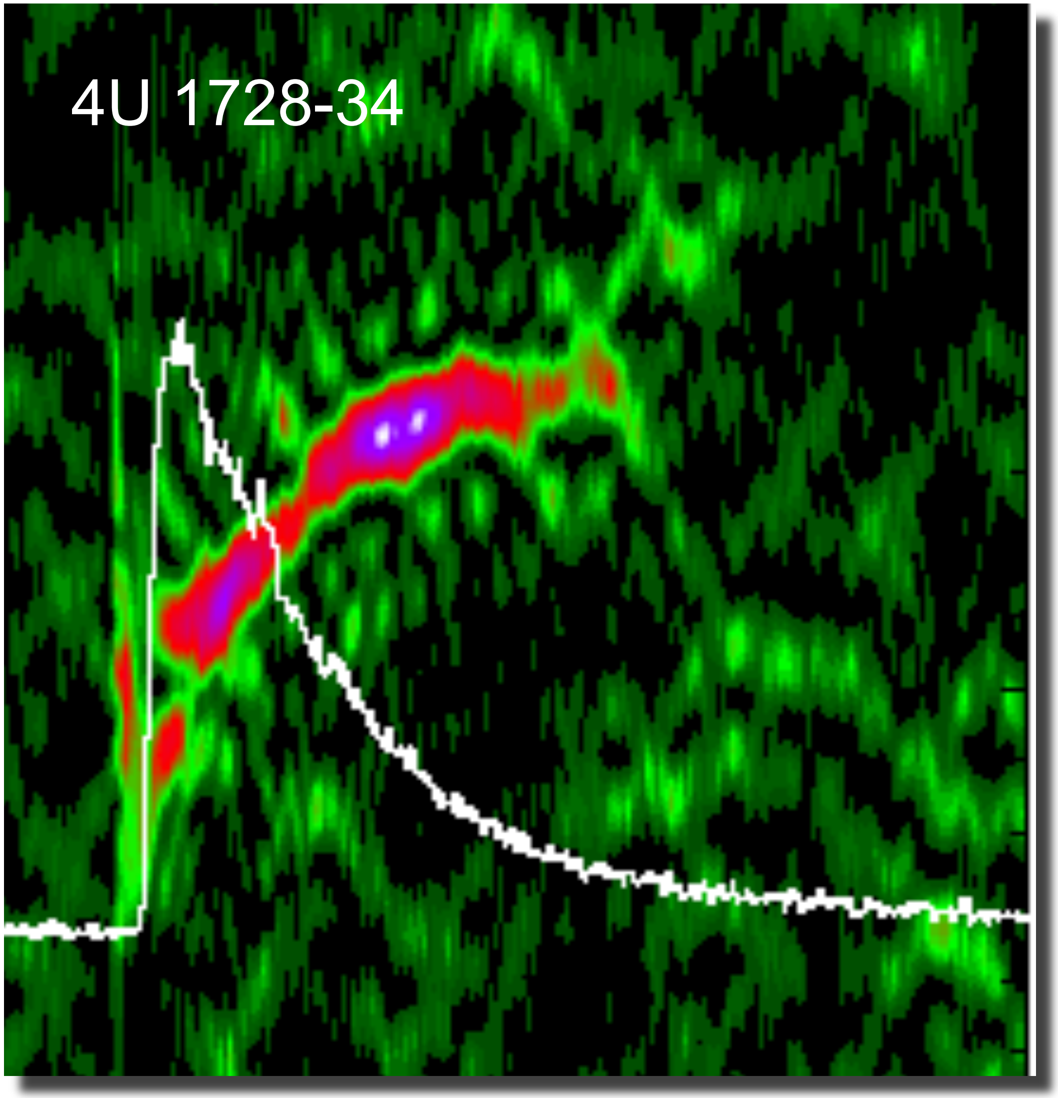

- Pulsations in the cooling tails can be as large as 15% (rms)
- If the whole surface is burned, what causes the flux asymmetry?
- Cooling time asymmetry is probably not large enough
- Oscillation modes (Heyl 2002 suggests *r*-modes; Piro & Bildsten 2005, Lee & Strohmayer 2005, Heyl 2005) ?

What Breaks the Symmetry?

- Global Oscillation modes could provide late time asymmetry.
- r-modes suggested by Heyl (2005), Lee & Strohmayer (2005). Are the modes unstable?
- Spitkovsky et al. suggest vortices “trapped” in zonal wind set up by differential cooling.
- Cumming (2005) finds dynamically unstable shear modes, associated with differential rotation, perhaps “self-excited” by bursts.
- Not settled yet.

Cumming (2005)

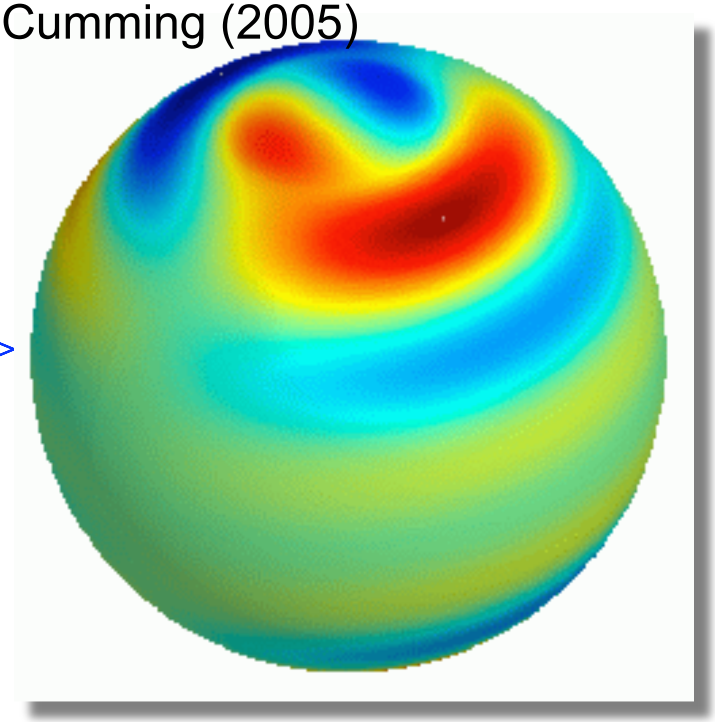

Puzzle # 1: Frequency Evolution of Burst Oscillations

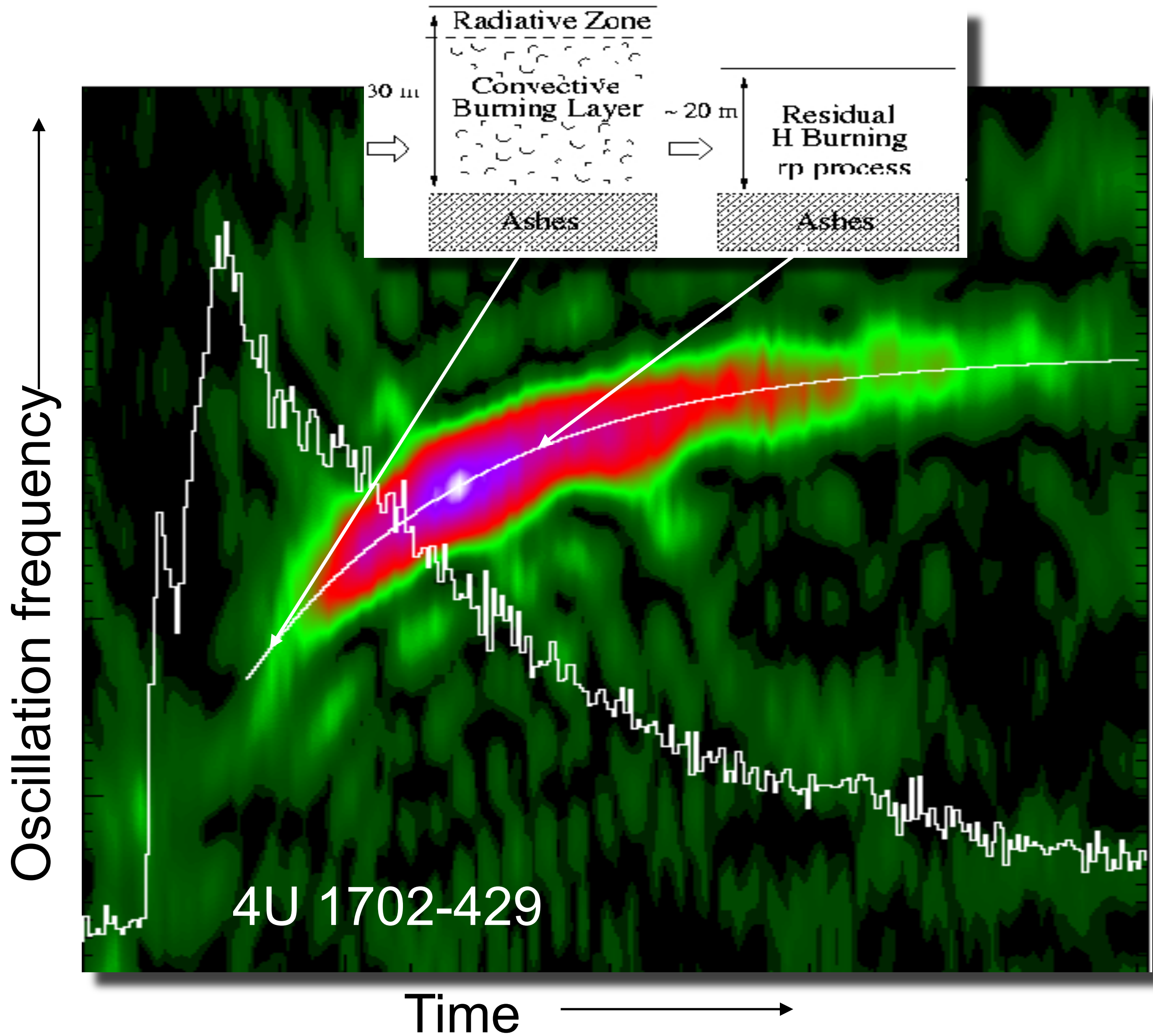

- Expanding layer slows down relative to bulk of the star.
- Change in spin frequency crudely consistent with expected height increase, but perhaps not for most extreme variations.
- X-ray burst expands surface layers by ~ 30 meters.

Spin Down of Burst Oscillations in 4U1636-53

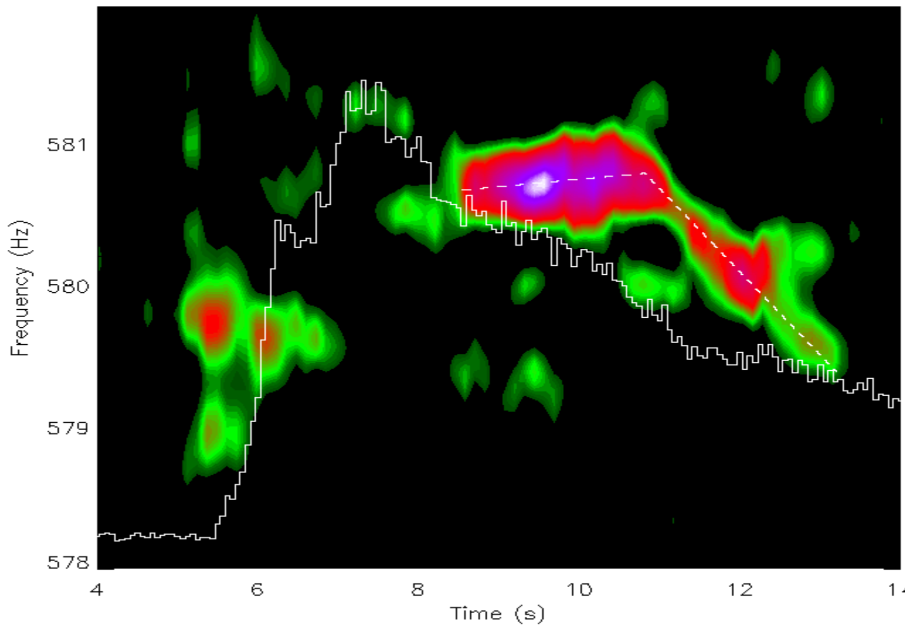

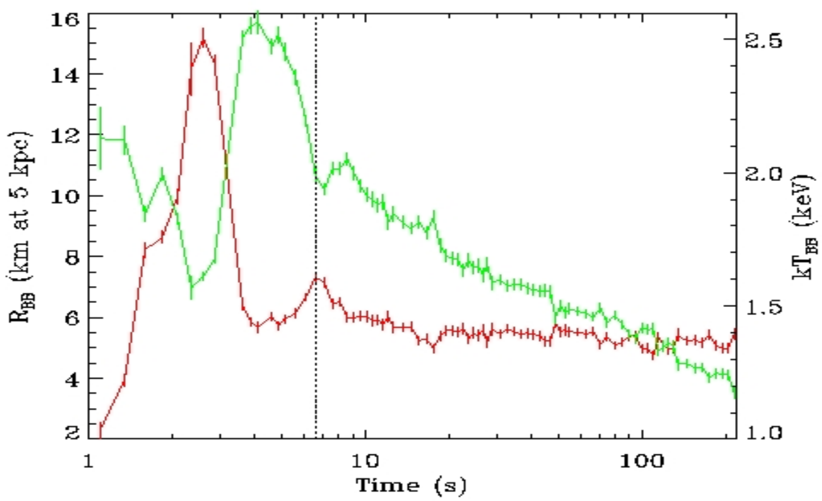

- A small fraction of bursts show episodes of spin down (Miller 1999; Strohmayer 1999).
- Spin down in 4U 1636-53 is associated with extended thermal tail and transition evident in spectral evolution.
- Magnitude of spin down may reflect an expansion of the surface layers by only 10 - 30 meters

Part 3
Superbursts, X-ray probes of NS

First Superburst from 4U 1735-44 (BeppoSAX/WFC)

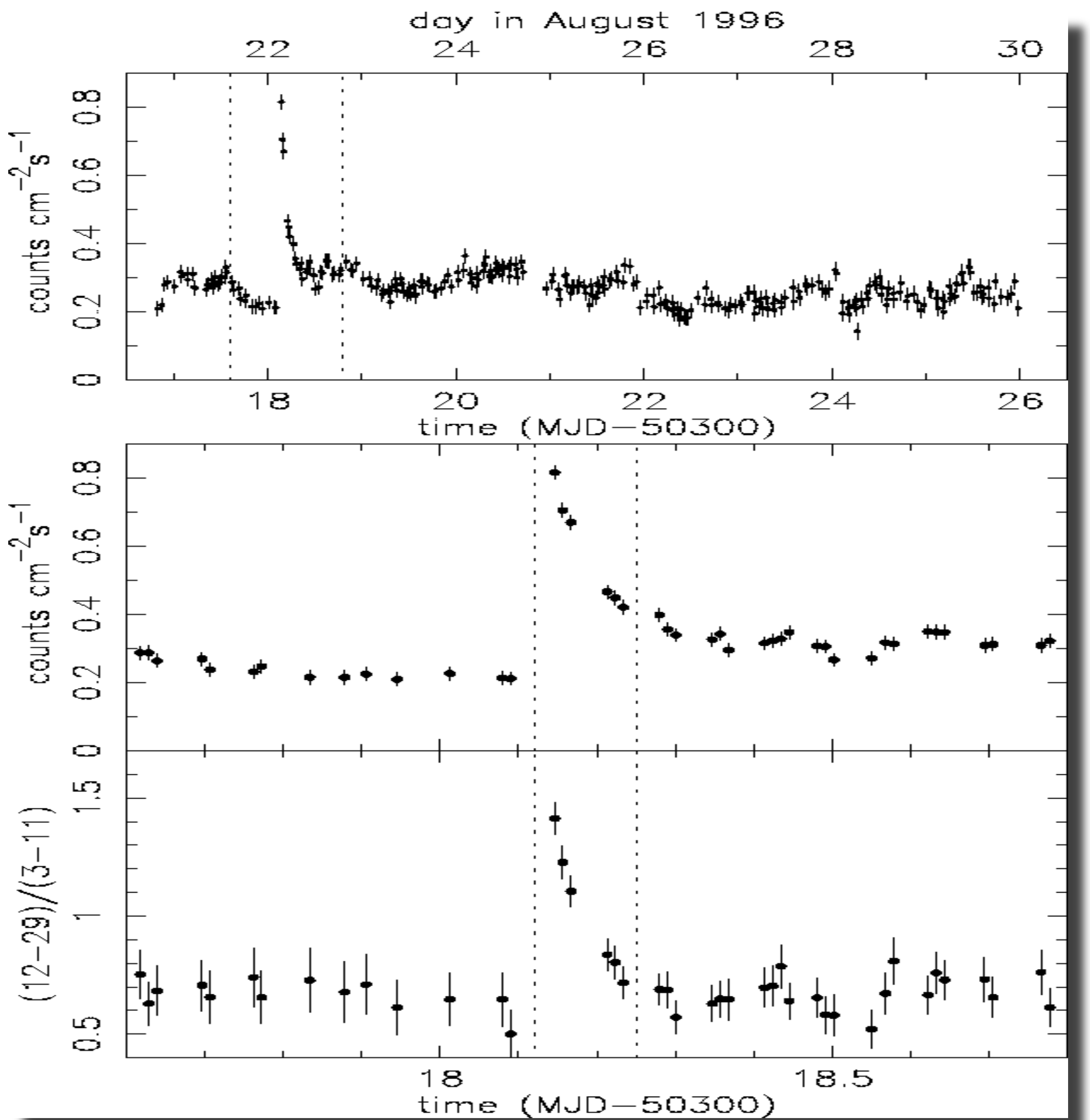

Cornelisse et al. (2000)

- Long, 3 - 5 hr flares seen to date from 9 low mass X-ray binaries (LMXB).
- Spectra consistent with thermal, show softening with time.
- Several superbursts from 4U 1636-53
- 1,000 x more energy than standard Type I bursts.

RXTE Observes Three Hour Thermonuclear Burst from a Neutron Star (4U 1820-30)

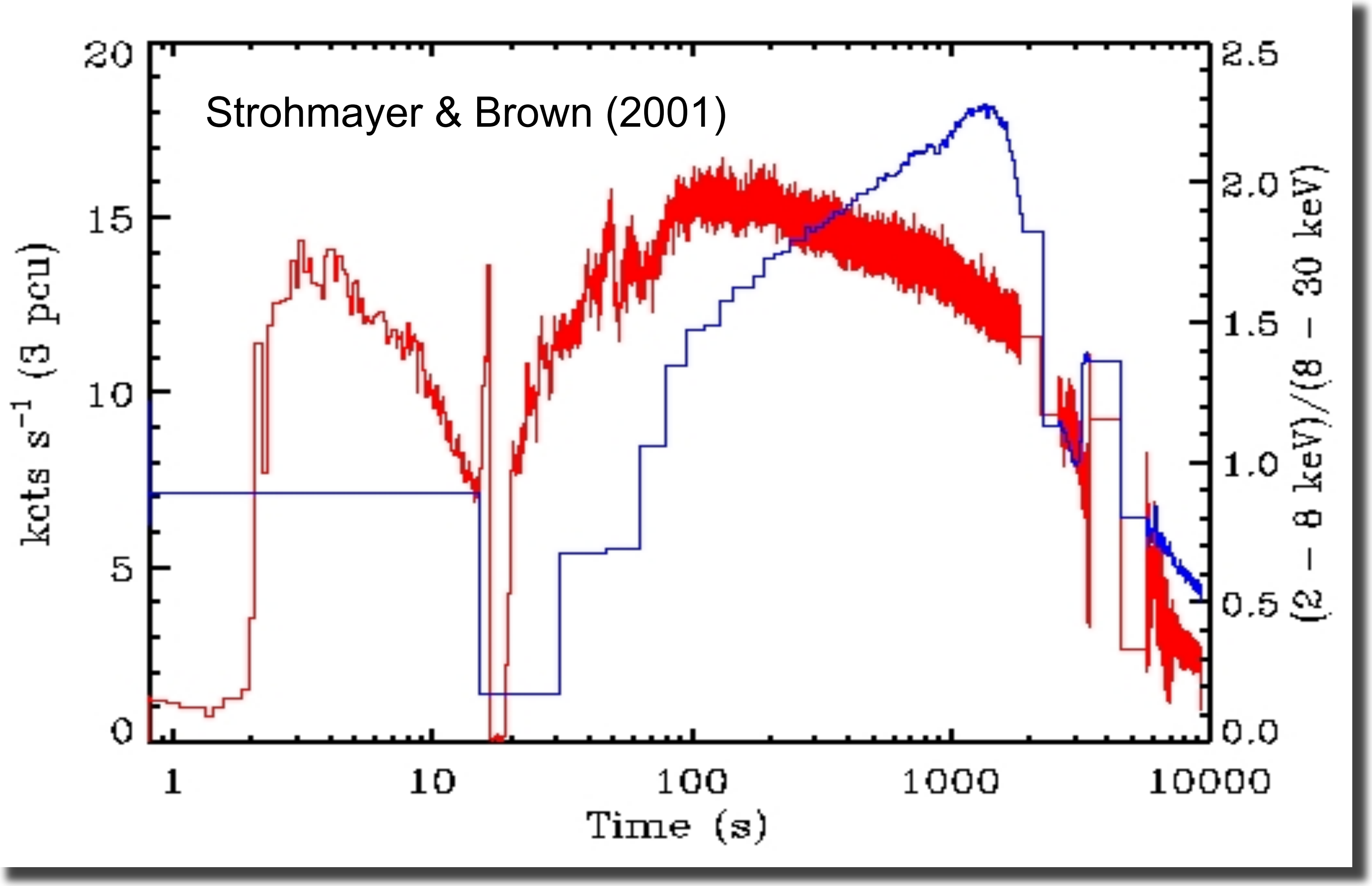

- Burst produced ~ 2 *x* 10^{42} ergs in X-rays, perhaps 10x more energy not seen (neutrinos; heat flowing into the crust).
- Energy source likely carbon burning at great depth (~10^{13} g cm^{-2}).

Superburst from 4U 1820-30: Carbon Production

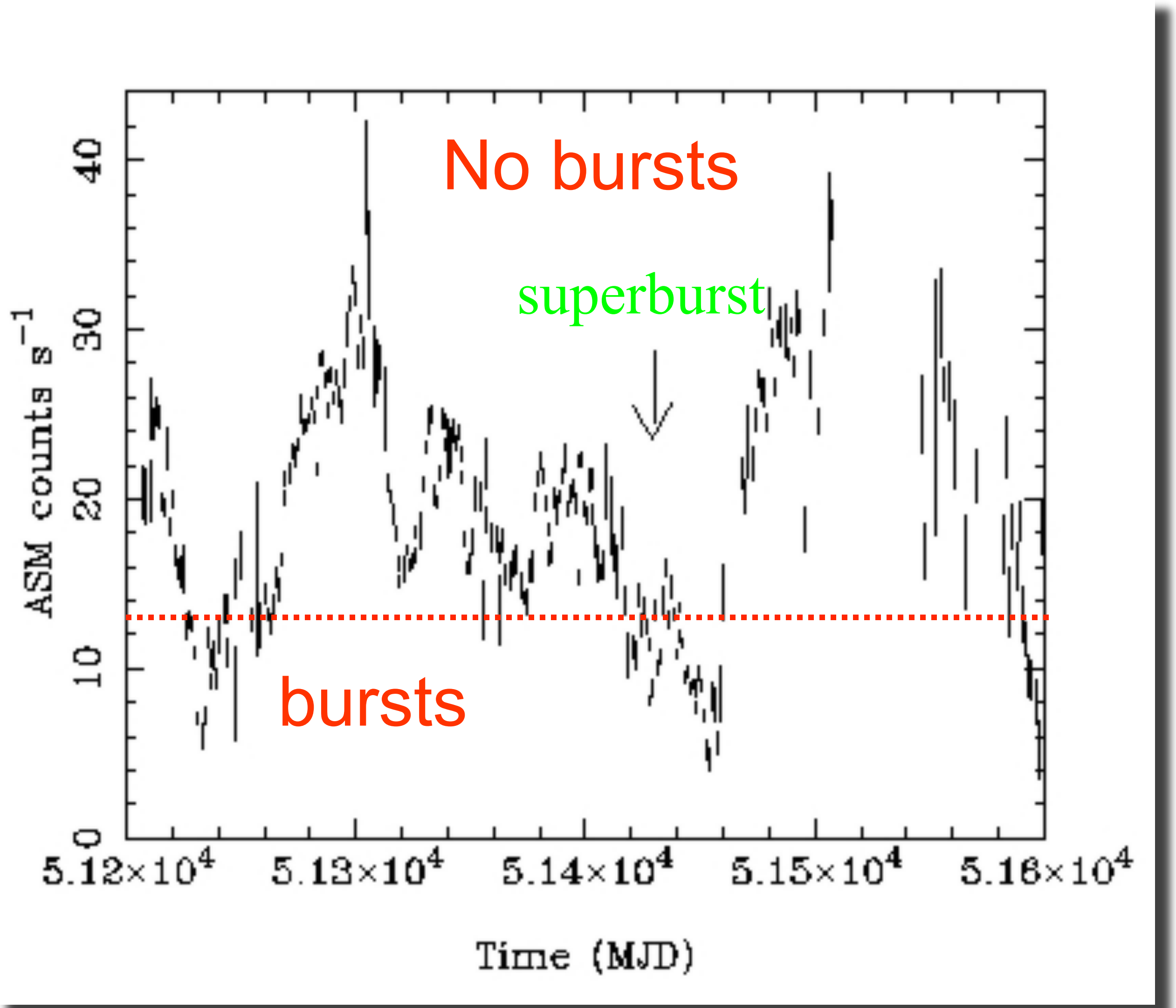

Strohmayer & Brown (2002)

- 4U 1820-30, He dwarf companion.
- Thermonuclear (helium) burning is stabilized at high accretion rates (ie. no normal bursts).
- Lower peak burning temperatures will likely synthesize sufficient Carbon.
- Higher temperature during unstable burning yields little Carbon

A Carbon "bomb" on a Neutron Star

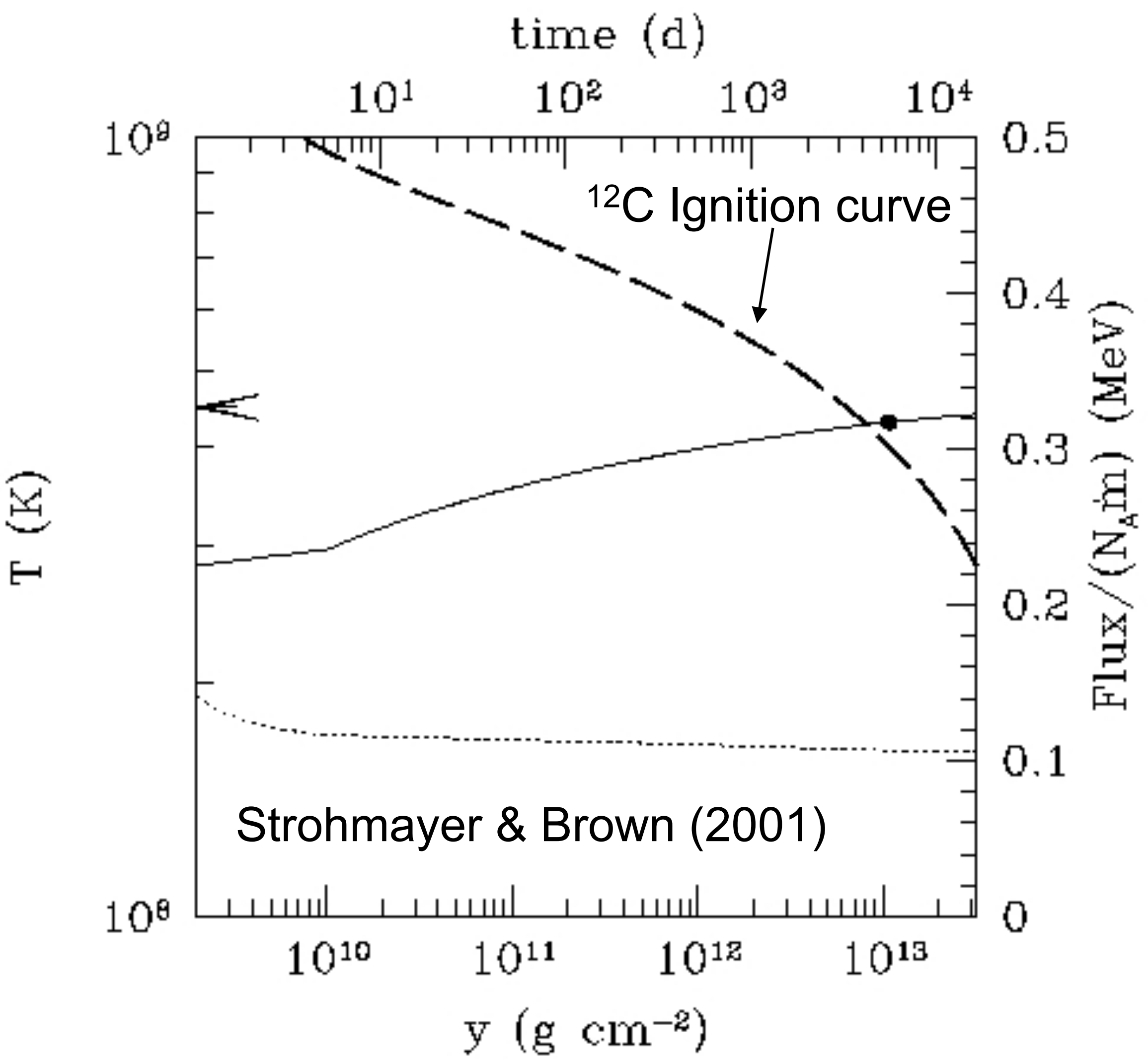

Carbon burning can supply total energy, recurrence time prediction ~ 12 years.

- Carbon produced during stable burning of accreted helium.
- Carbon ignites at 10^{13} g cm^{-2}. Total energy is ~10-20 times greater than X-ray fluence.
- Significant energy loss to neutrinos, energy will flow inward to be released on longer timescale.

likely 2nd superburst from 4U 1820-30 seen 10.5 yrs later (In 't Zand et al. 2011)

Superburst Probes of Accretion Disks

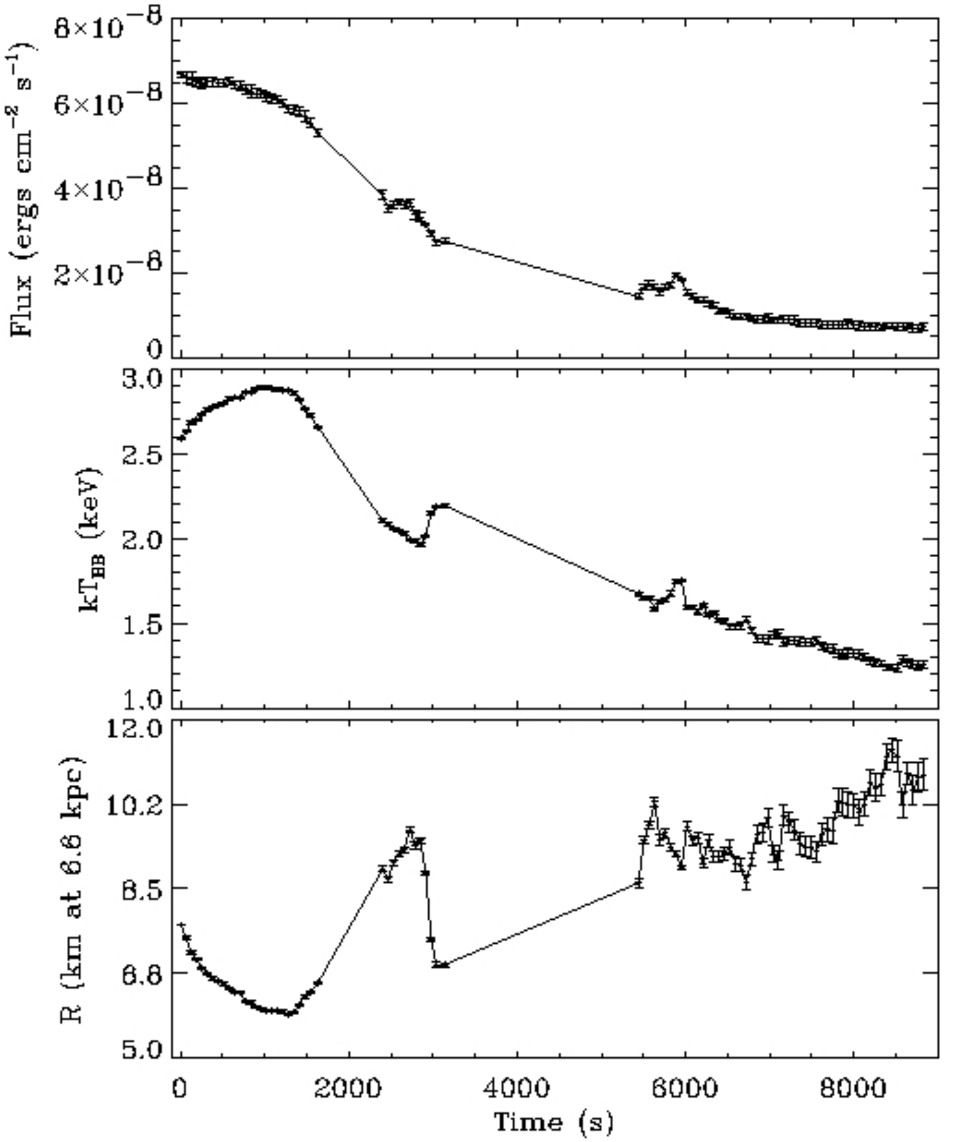

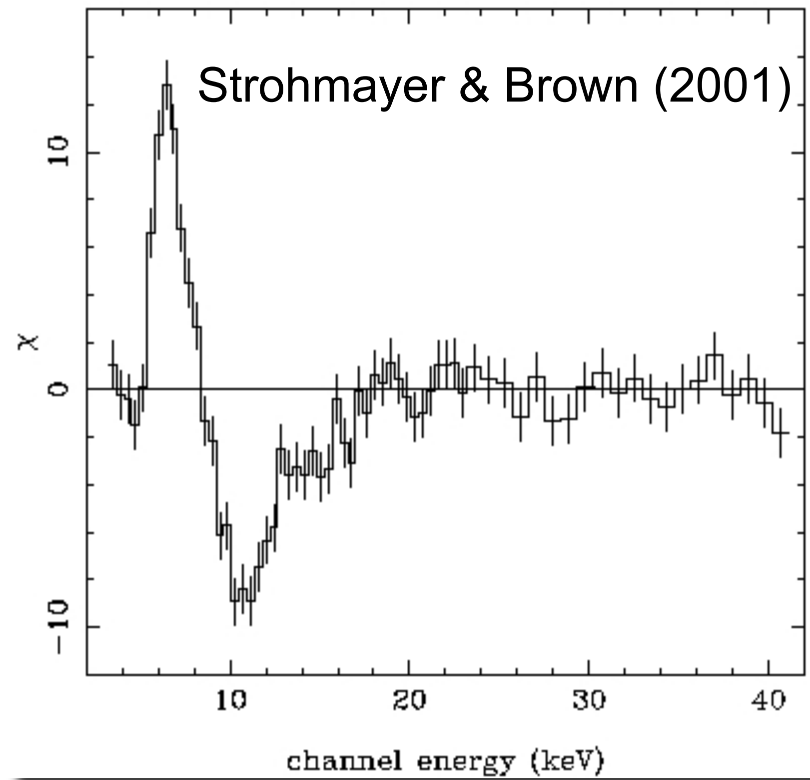

- Peak flux consistent with Eddington limit from neutron star.
- Broad ~6 keV line and ~9 keV edge from reflection off inner disk.
- New probes of disks and neutron star.

Superburst from 4U 1820-30: Disk Reflection

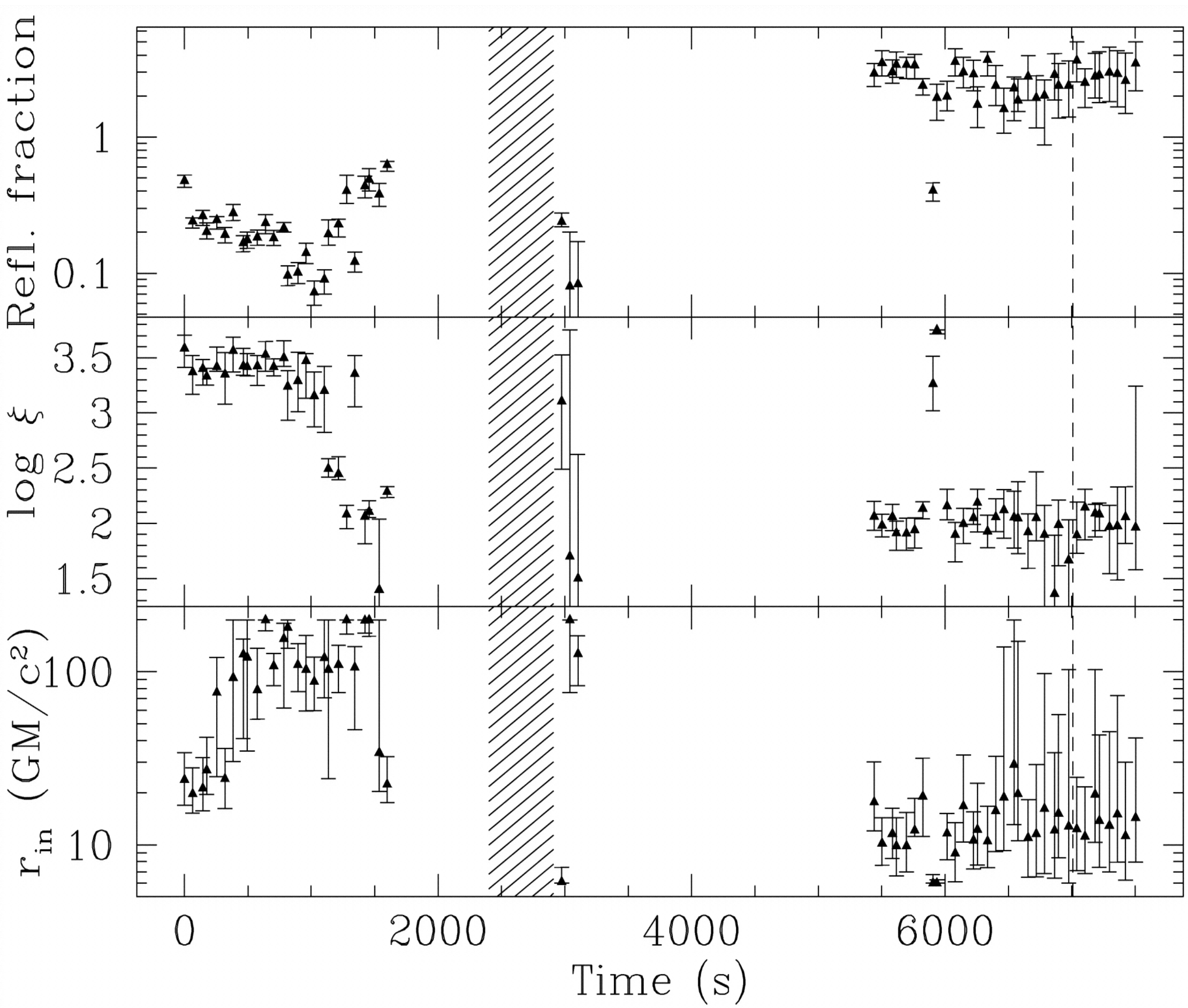

Ballantyne & Strohmayer (2004)

- Discrete spectral components likely due to reflection of burst flux from disk.
- Broad Fe Kα line and smeared edge.
- Line and edge parameters vary significantly through burst.
- Broad Fe line gives evidence for relativistic disk.

Superbursts: Burst Quenchning

- Superbursts heat ocean and "quench" H/He bursting following the superburst. Evolution sensitive to cooling and composition in the ocean.
- New modeling (Keek et al. 2012) shows diverse behavior depending on accreted composition. Relatively short quench times.
- Data are unfortunately not very constraining, superbursts very rare, and sparse observational coverage.

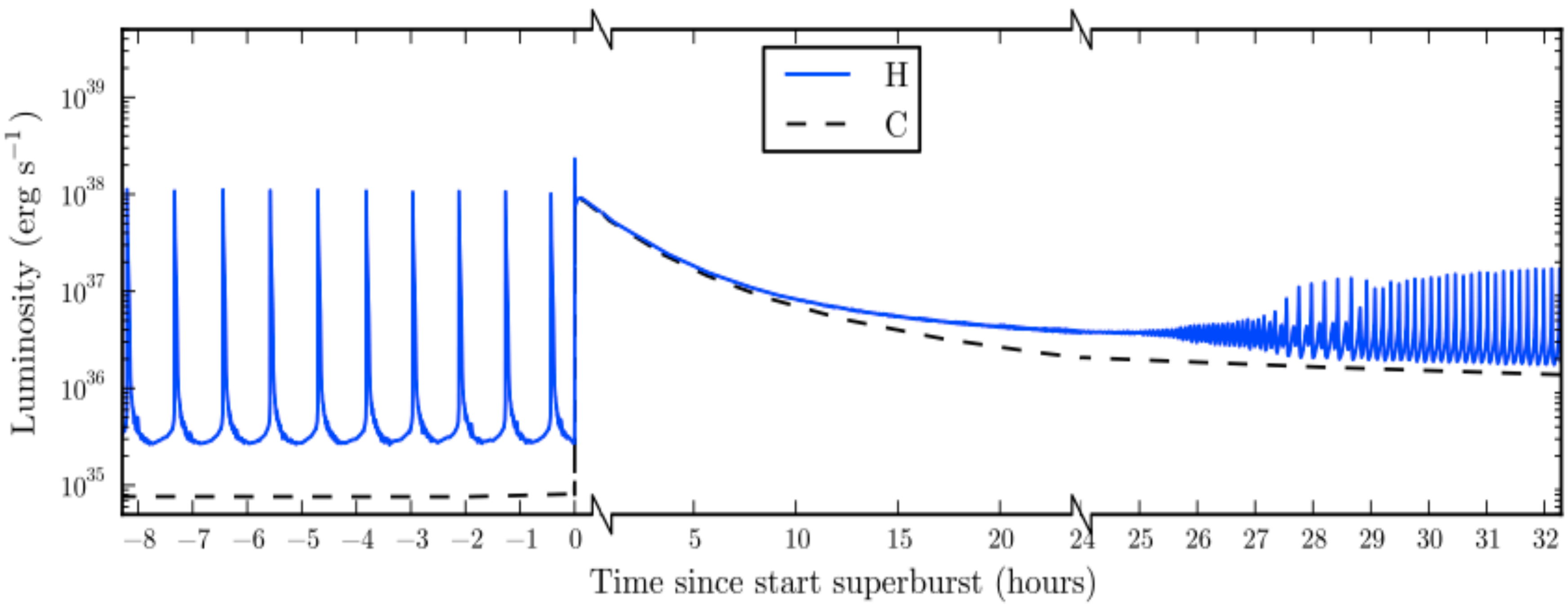

Superbursts: Current Status and Theoretical Concerns

- Carbon Production: If too much H around, Carbon destroyed, concern for H accretors. But stable burning does produce carbon, and α values for SBs suggests there is stable burning.
- Carbon ignition: Fits to cooling light curves gives ignition column, energy. Is ocean-crust hot enough to ignite at that depth? Revised deep-crustal heating (Gupta et al. 2007) helps, but current models still seem to under predict temperatures needed (Keek et al. 2008)

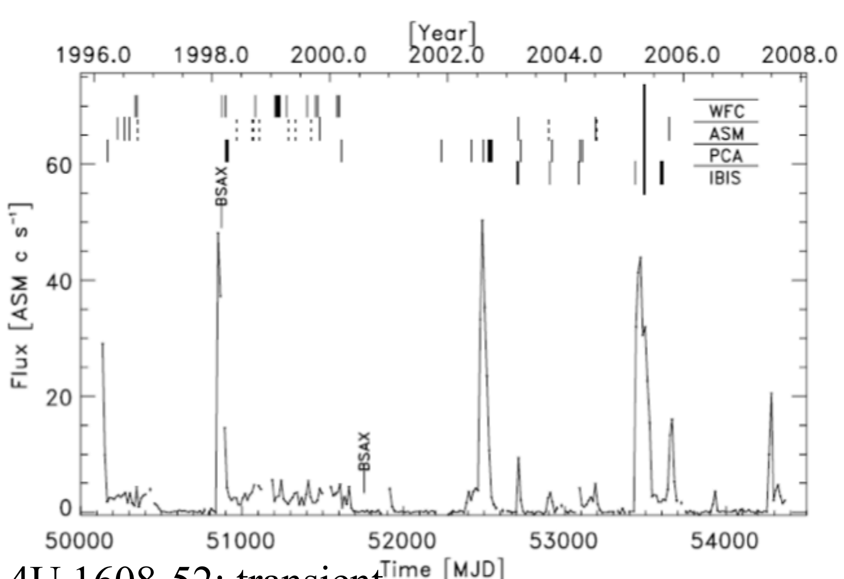

4U 1608-52: transient

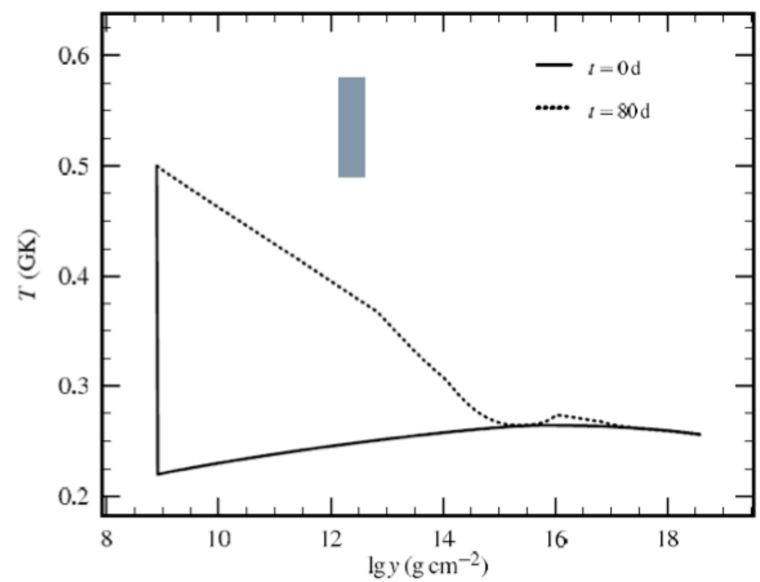

Pulsar Mass, and Radius Measurements

Detection of pulsars in binary systems; typically gives measurement of the orbital period, P_b, and a_x sin i. This gives the mass function:

$$f_x = \frac{4\pi^2 (a_x \sin i)^3}{G P_b^2} = \frac{(M_c \sin i)^3}{(M_x + M_c)^2}$$

Gives minimum mass of the companion star, but not neutron star mass, M_x (single-lined spectroscopic binary). Radial velocity measurements (optical) of the companion. This can give you the mass ratio, $q = m_x/m_c$, but sin i is still unknown (usually difficult). Other possibilities; Post-newtonian effects (shapiro delay);

$$\Delta t_s = -2GM_c/c^2 \log(1 - \sin i \sin \phi)$$

Shapiro delay: Not yet measured in an X-ray pulsar

Pulsar Mass, and Radius Measurements

additional constraints possible; eclipse timing and Roche lobe accretion.

$$\cos^2 i + \sin^2 i \times \sin^2(\pi T_{\rm ecl}/P_b) = \sin^2(\theta/2)$$

$$R_c = a_{\rm tot}\sin(\theta/2)$$

Eclipse timing combined with pulsar timing is very powerful. A mass ratio measurement would yield both component masses and the inclination. Shapiro delay measurement would also provide a full mass solution. Eclipses require large i, so also good for Shapiro.

Accreting X-ray Pulsar timing, including eclipses!

New Accreting Millisecond Pulsar: Swift J1749.4-2807

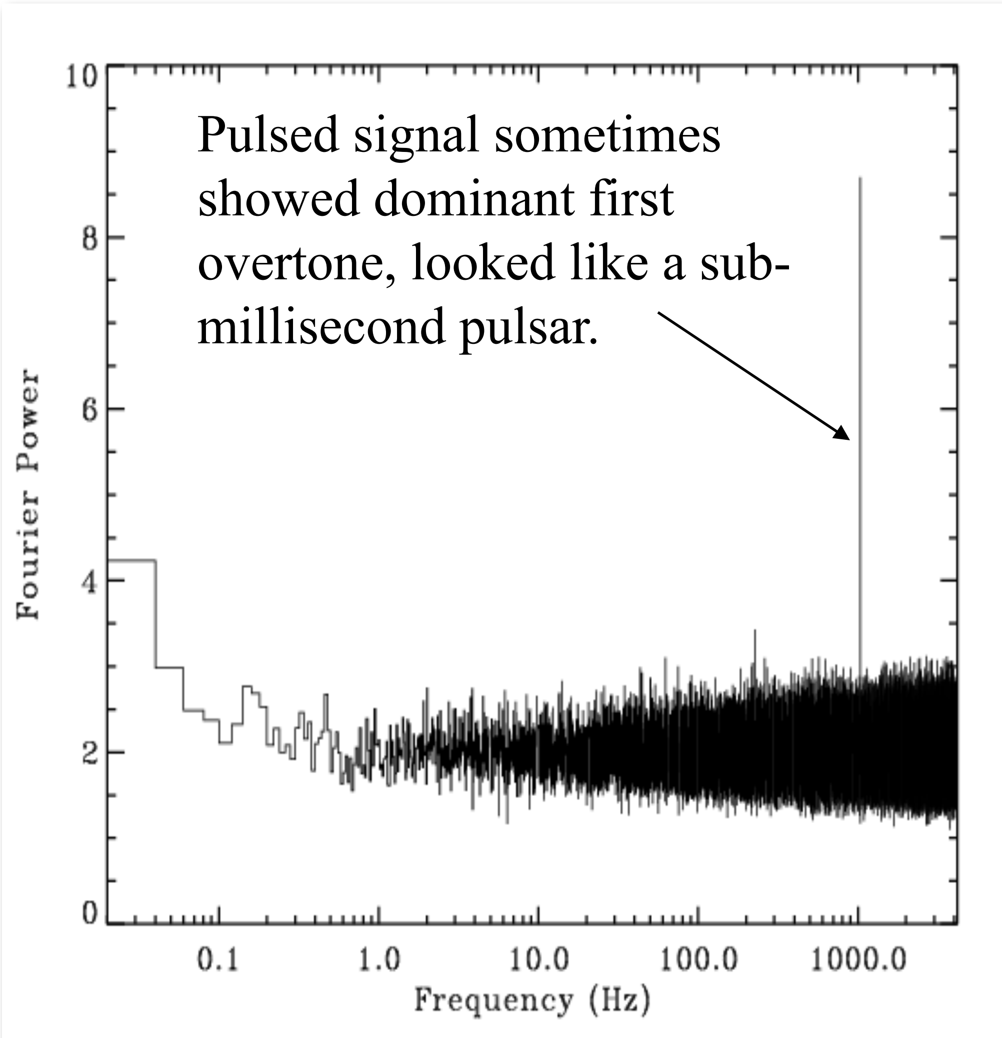

- RXTE observations detect 518 Hz pulsar, with strong, sometimes dominant first overtone (1035.84 Hz, Altamirano et al. 2010).
- 8.817 hr circular orbit, vsini = 112.8 km/sec (Belloni et al, 2010; Strohmayer & Markwardt 2010

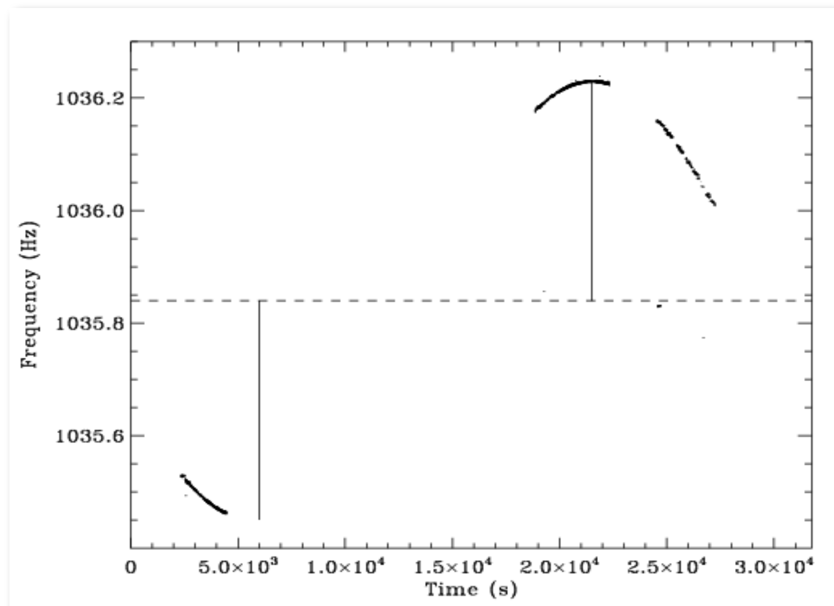

New Accreting Millisecond Pulsar: Swift J1749.4-2807

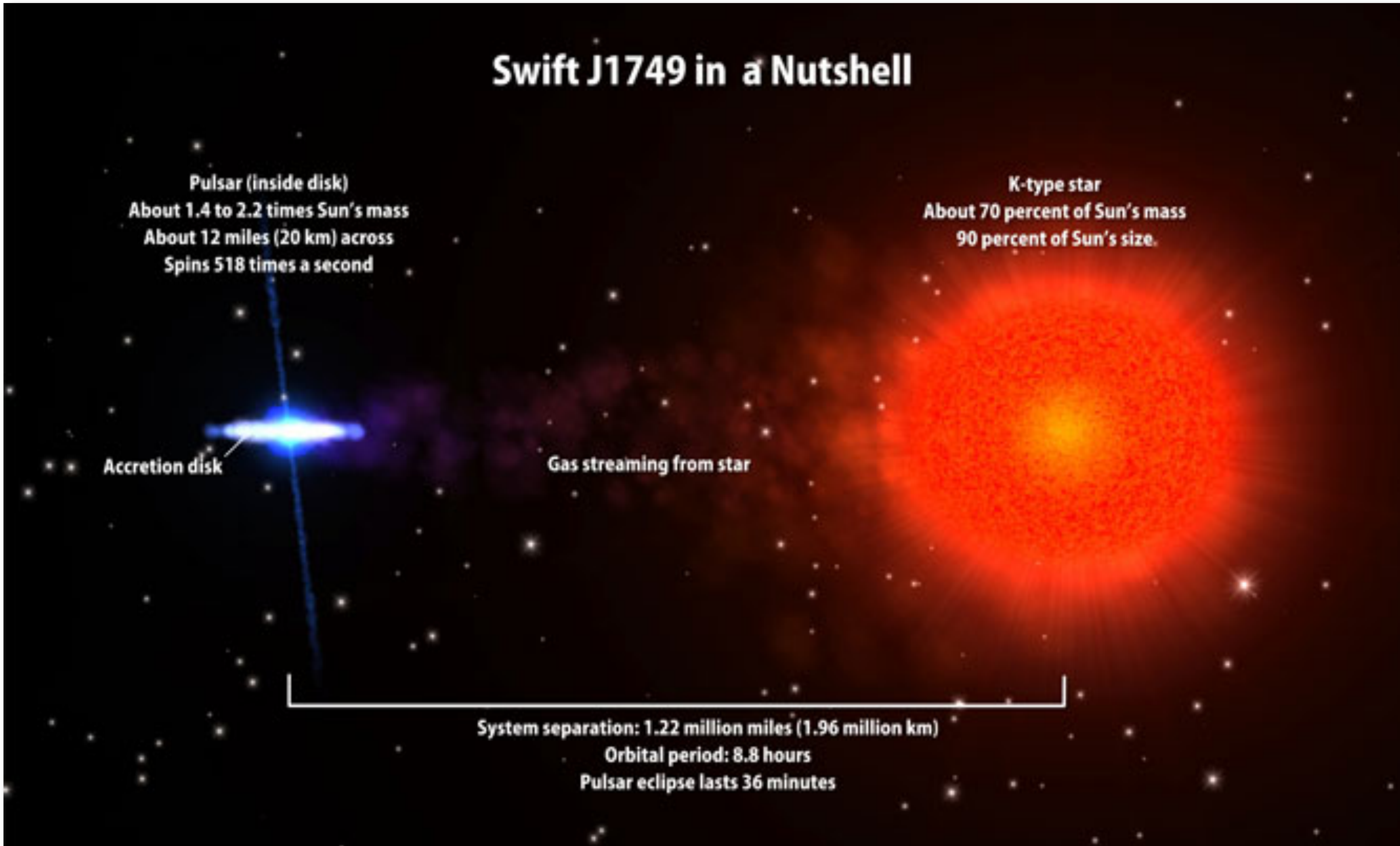

- Source discovered in 2006 when X-ray burst detected with Swift/BAT.
- New outburst detected in April 2010 (INTEGRAL, Swift).

Swift J1749: First Eclipsing AMXP!

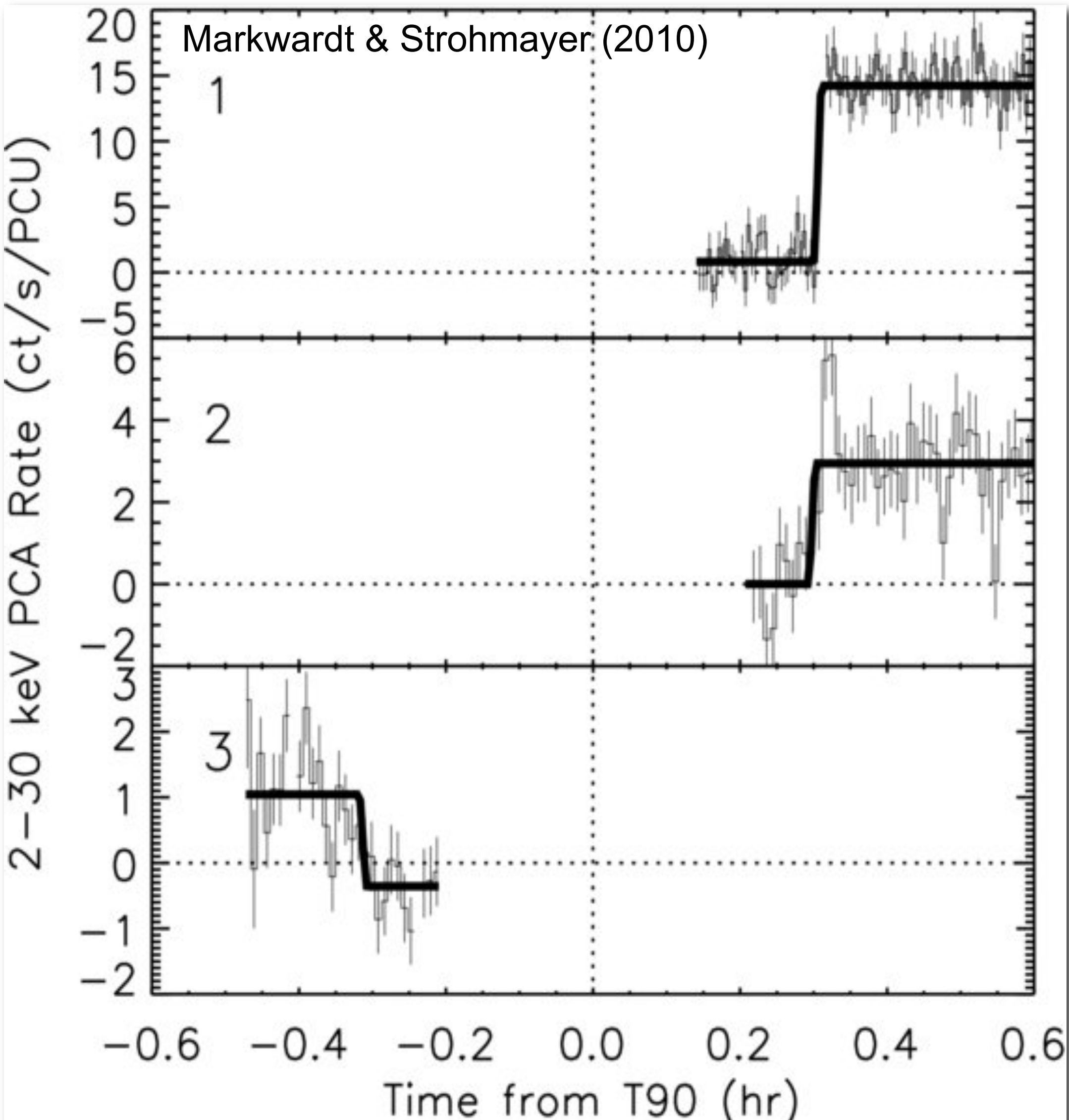

- Eclipse features evident in the PCA X-ray light curves.
- Features are symmetric about orbital phase of superior conjunction of the NS, as expected for eclipses of NS by the donor.
- Two egresses and one ingress observed.
- Eclipse duration of 36.2 minutes, 6.85% of the orbital period.
- Eclipse timing tightly constrains inclination and properties of the donor.

Shapiro Delay in Swift J1749?

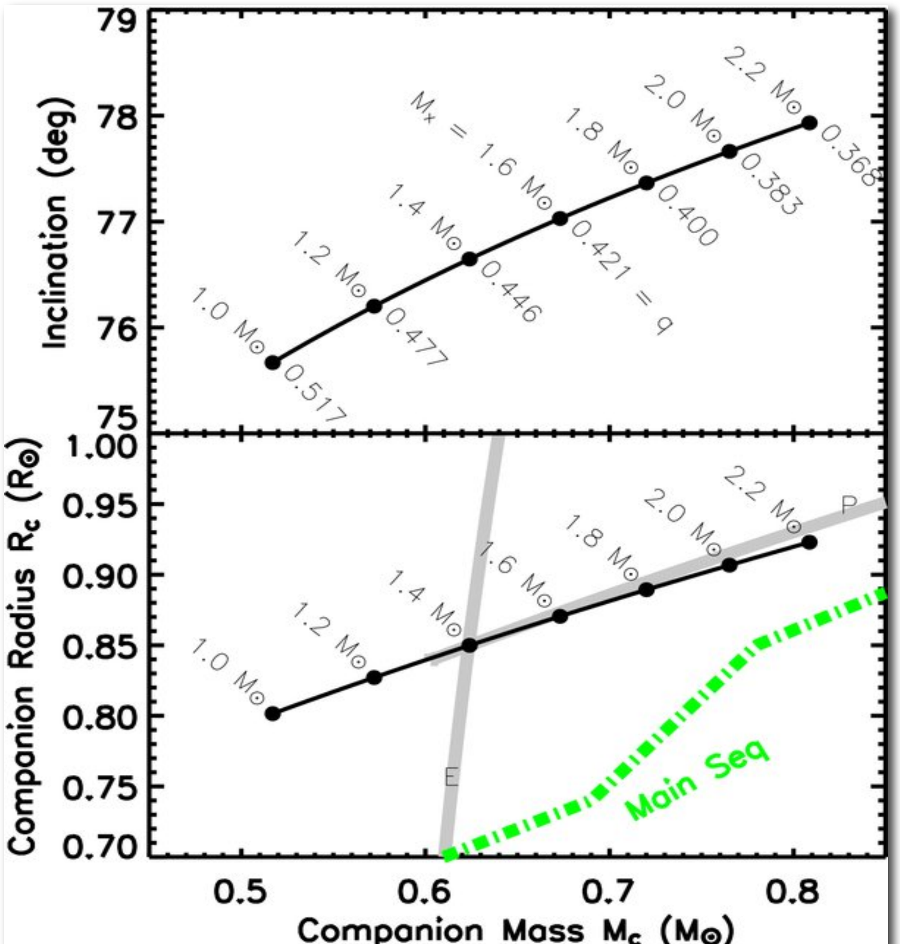

• High inclination, and relatively massive donor, Shapiro delay ~21 u-sec is within RXTE's timing uncertainty.

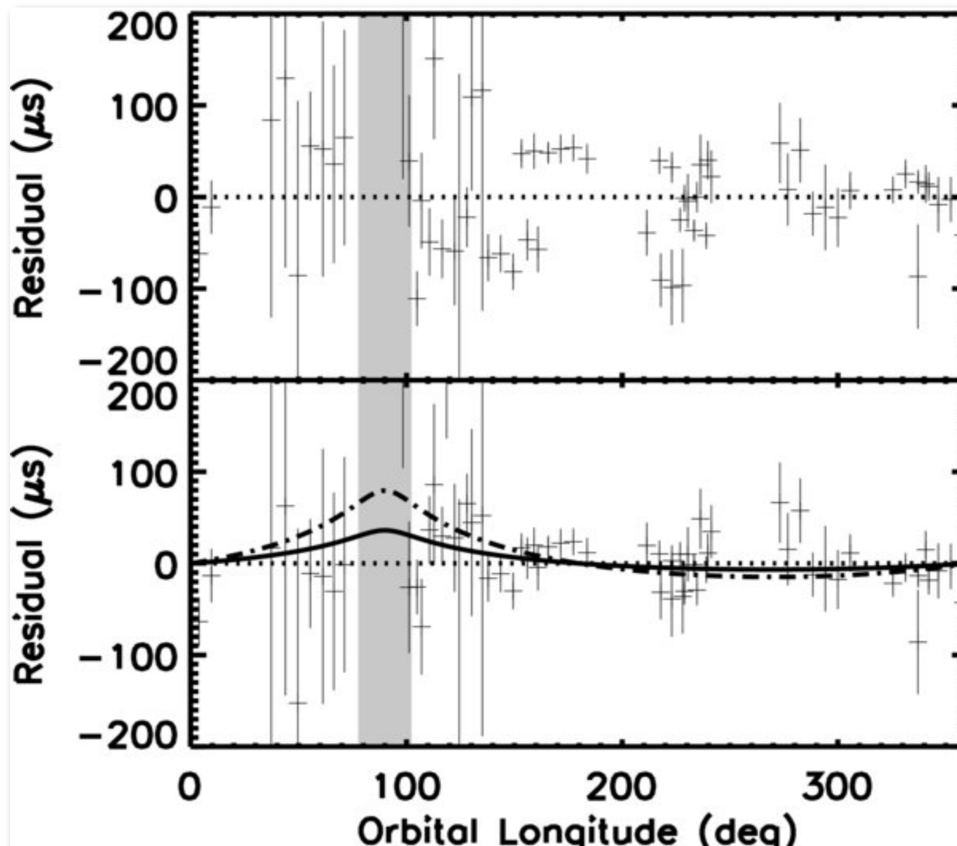

• Joint eclipse and pulse timing tightly constrain the system.

Burst Oscillations Probe the Structure of Neutron Stars

- Pulse strength and shape depends on M/R or ‘compactness’ because of light bending (a General Relativistic effect).
- More compact stars have weaker modulations.
- Pulse shape (harmonic content) depends on relativistic rotational speed, which depends on R (ie. spin frequency known).

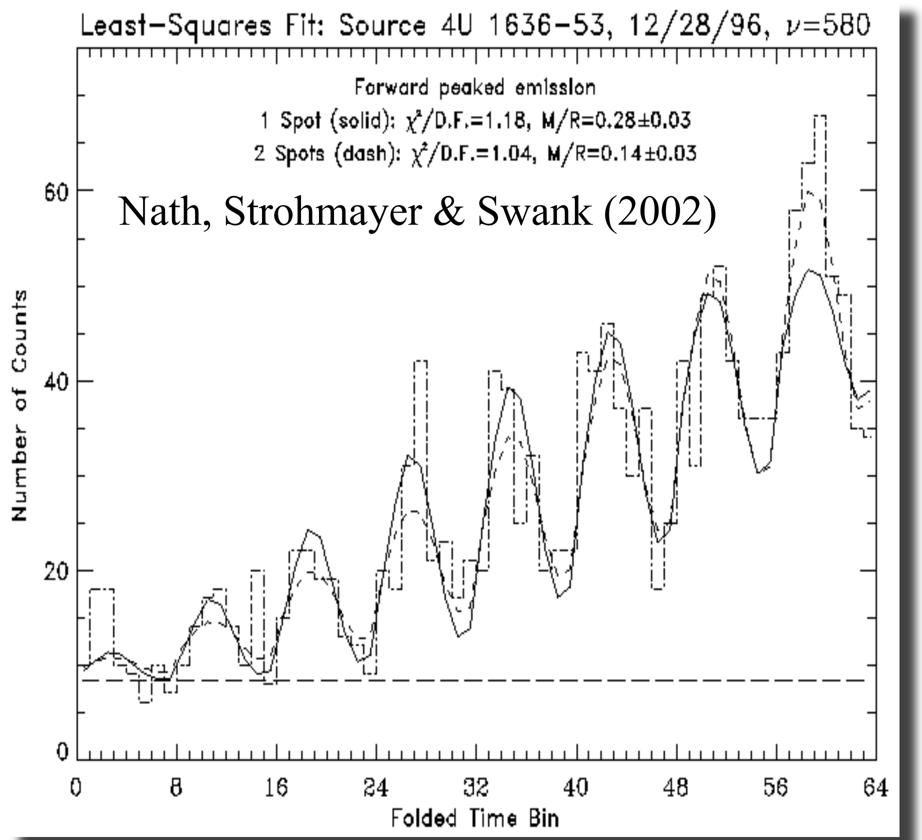

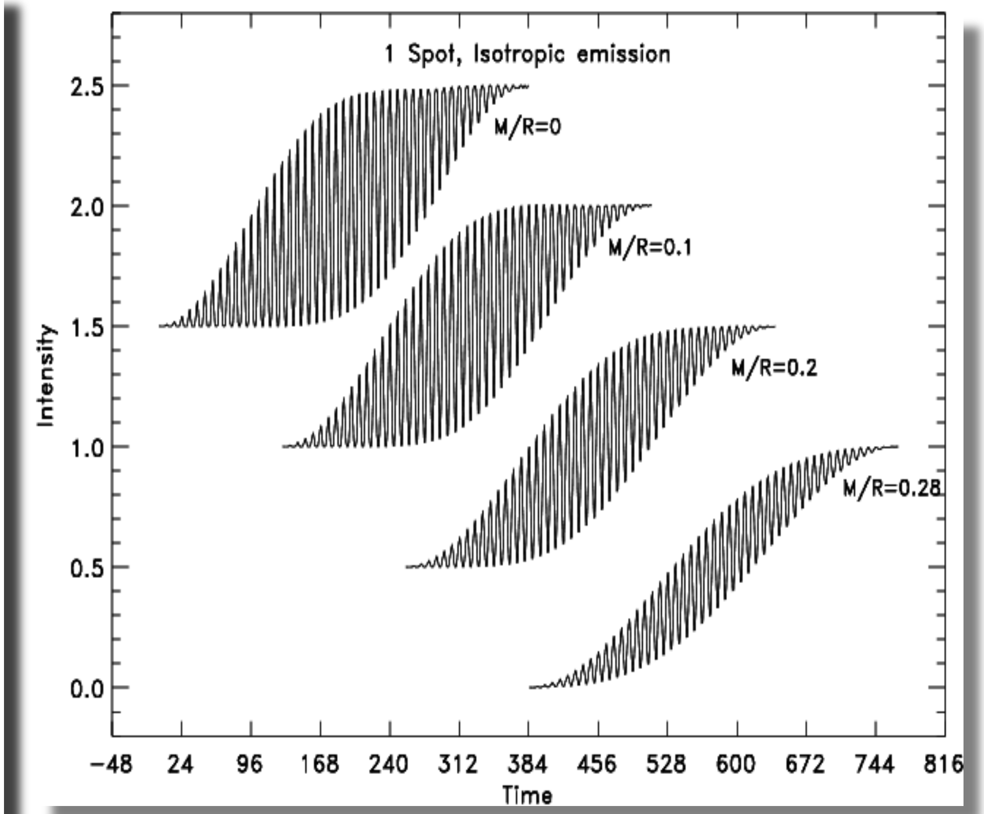

Rotational Modulation of Neutron Star Emission: The Model

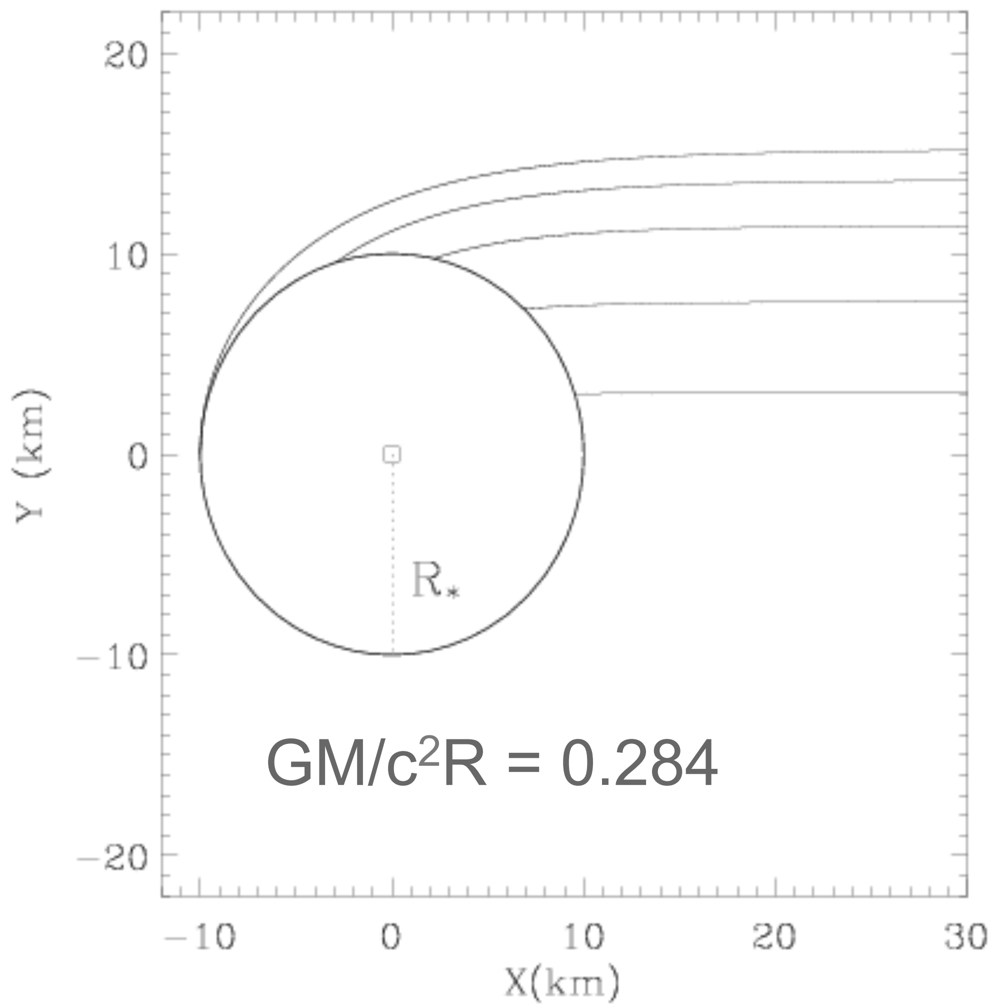

- Gravitational Light Deflection: Kerr metric with appropriate angular momentum.
- Gravitational redshift
- Rotational doppler shifts and aberration of the intensity.
- "Beaming" of intensity in NS rest frame.
- Arbitrary geometry of emission regions.
- Self-consistent neutron star structure (several EOSs

Bhattacharyya, Strohmayer, Miller & Markwardt (2005).

Mass – Radius Constraints: Recent Results: XTE J1814-338

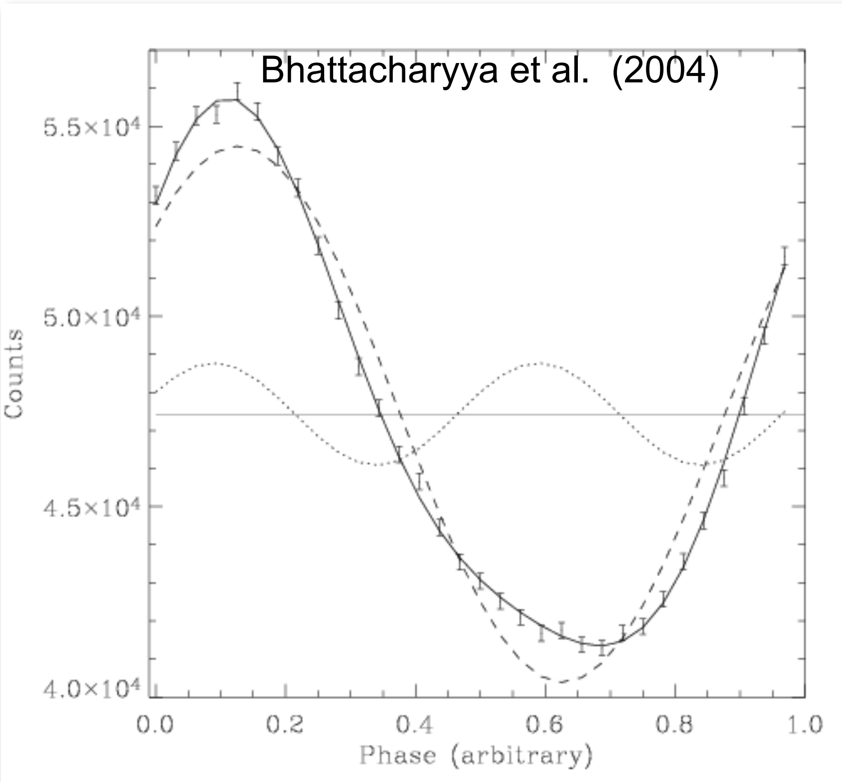

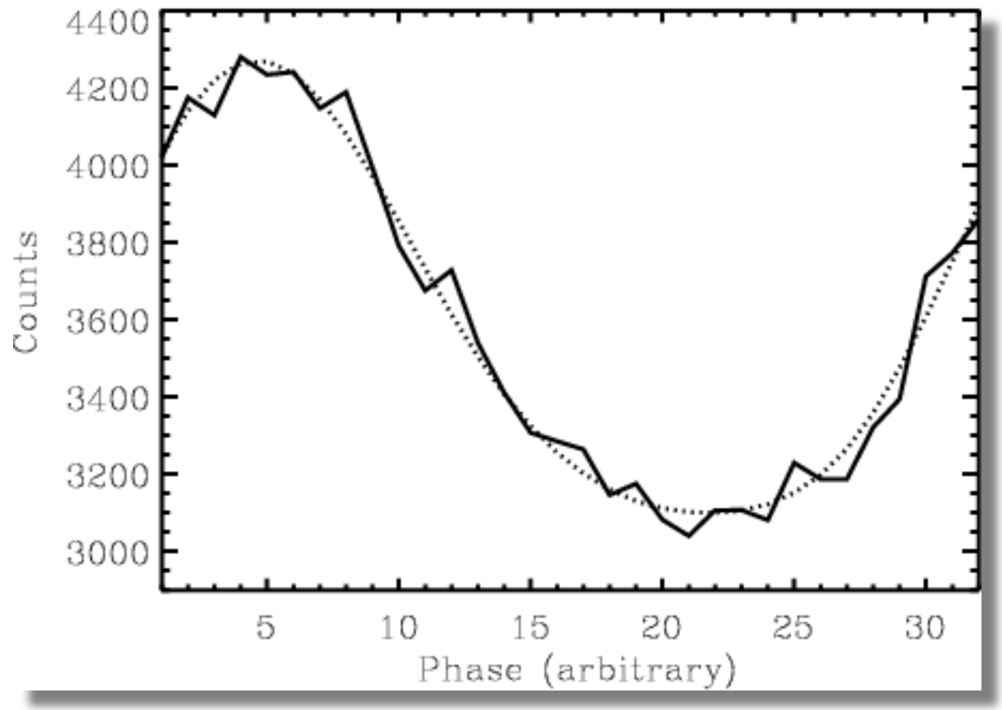

- 27 X-ray bursts from XTE J1814-338 (ms pulsar).
- High signal to noise burst oscillation profiles, with first ever harmonics.
- Phase resolved profiles in 5 energy bands.

- Use Bayesian method, determine likelihoods for each combination of parameters (uniform priors).
- Parameters: R/M, spot location and size (2), beaming exponent, observers inclination angle. Fix surface temperature (BB).

Compactness limits from pulse fitting in XTE J1814-338

- Results for two representative EOSs (soft and stiff).
- Model provides an acceptable fit in the χ^2 sense.
- R/M distributions peak in "reasonable" range. R/M > 4.2.
- Likelihoods do not yet favor a particular EOS.

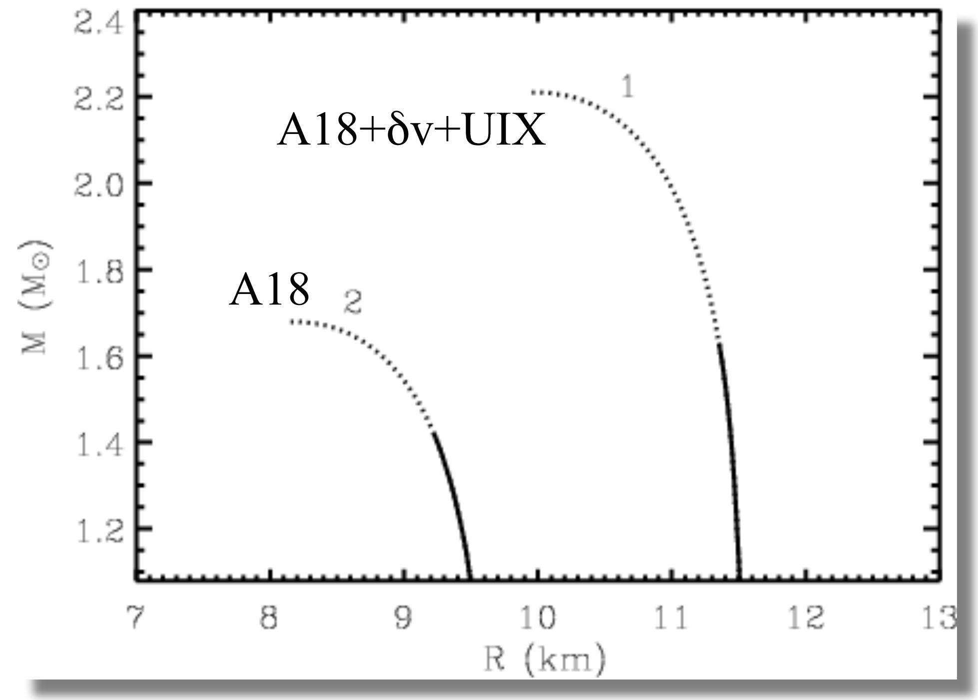

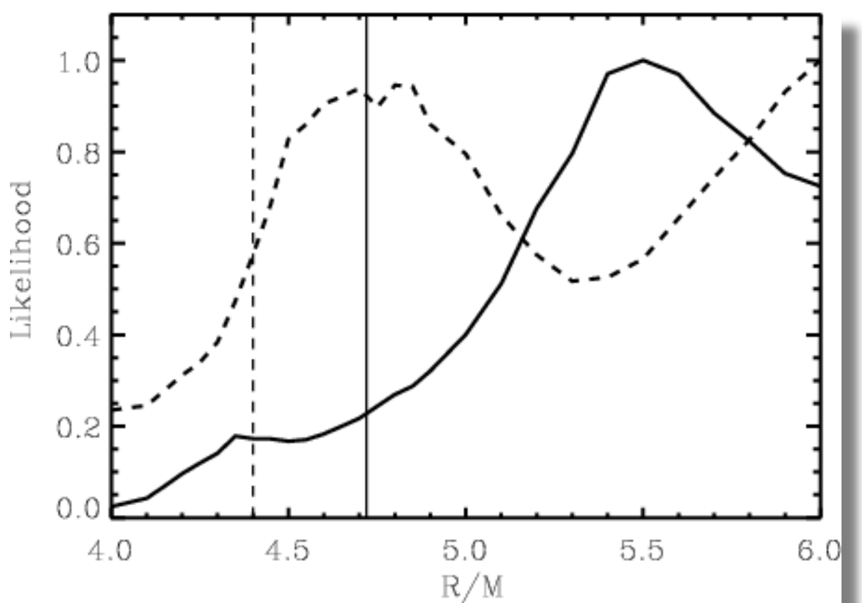

- Lattitude of hot spot near rotational equator (+- 30 degrees).
- Moderately low inclination (30 – 50 degrees)
- Some evidence for spot size evolution during outburst.

Mass – Radius Constraints: Persistent Pulse Profiles

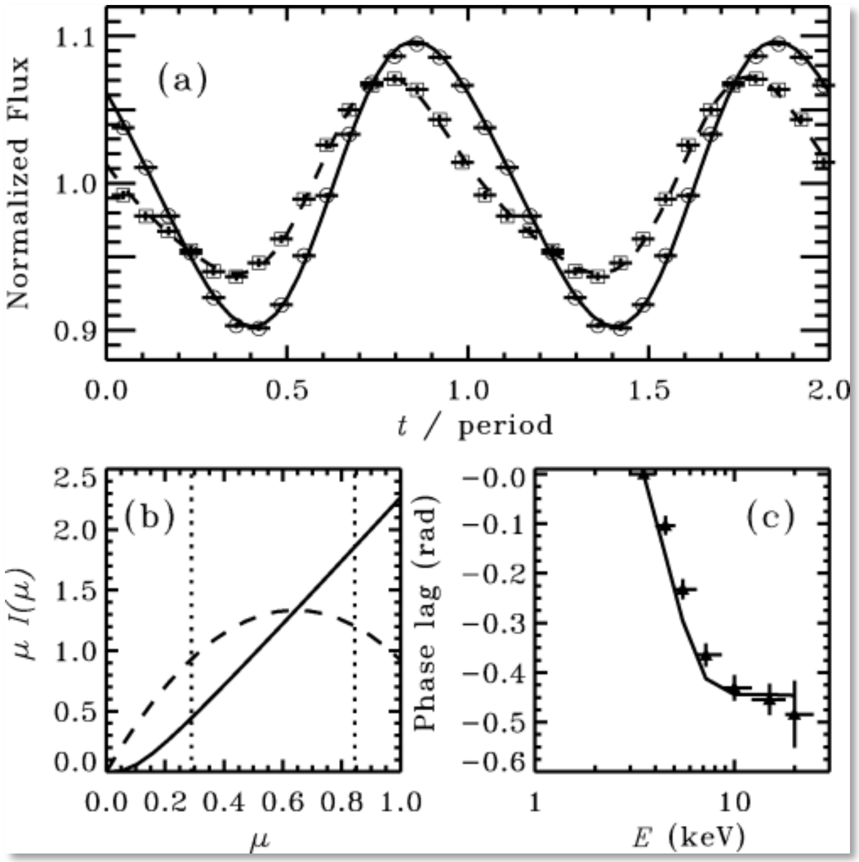

- Comparison of constraints from SAX J1808.4-3658 (Poutanen & Gierlinski 2003, red), and XTE J1814-338 (Bhattacharyya et al. 2005, green line).

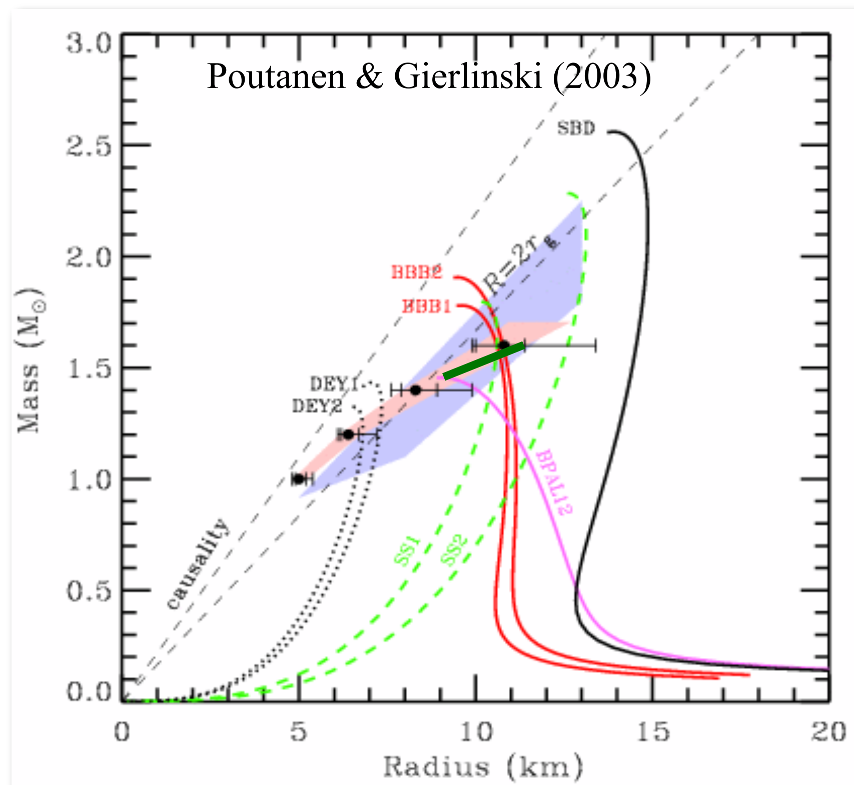

- Two component model: Thermal spot (soft); comptonized (hard).
- Very high signal to noise pulse profile.

Simulations for ~20x RXTE Collecting Area (LOFT)

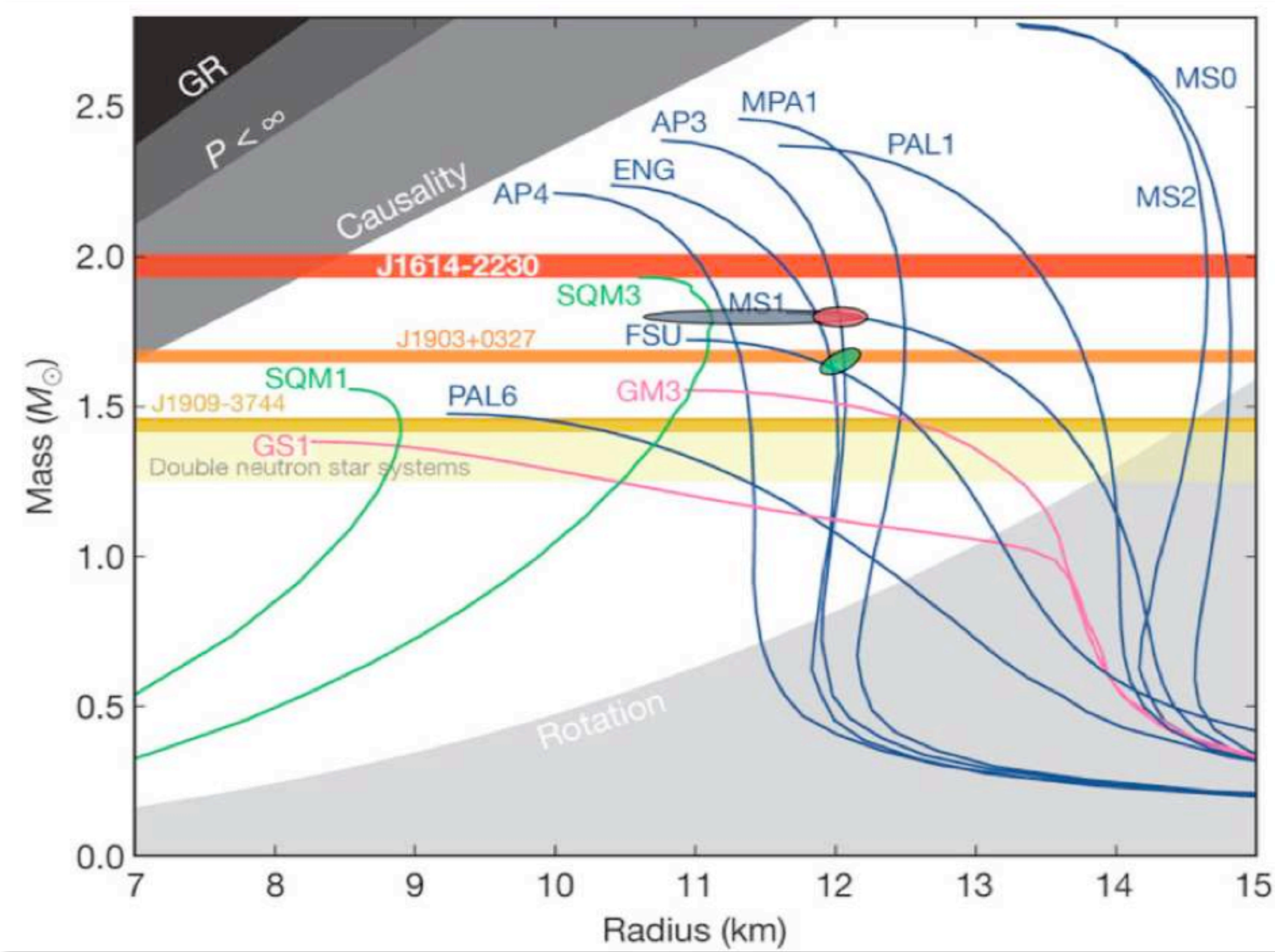

Caveat: statistical constraints, systematic modeling needs further investigation

Magnetar Oscillations in Giant Flares

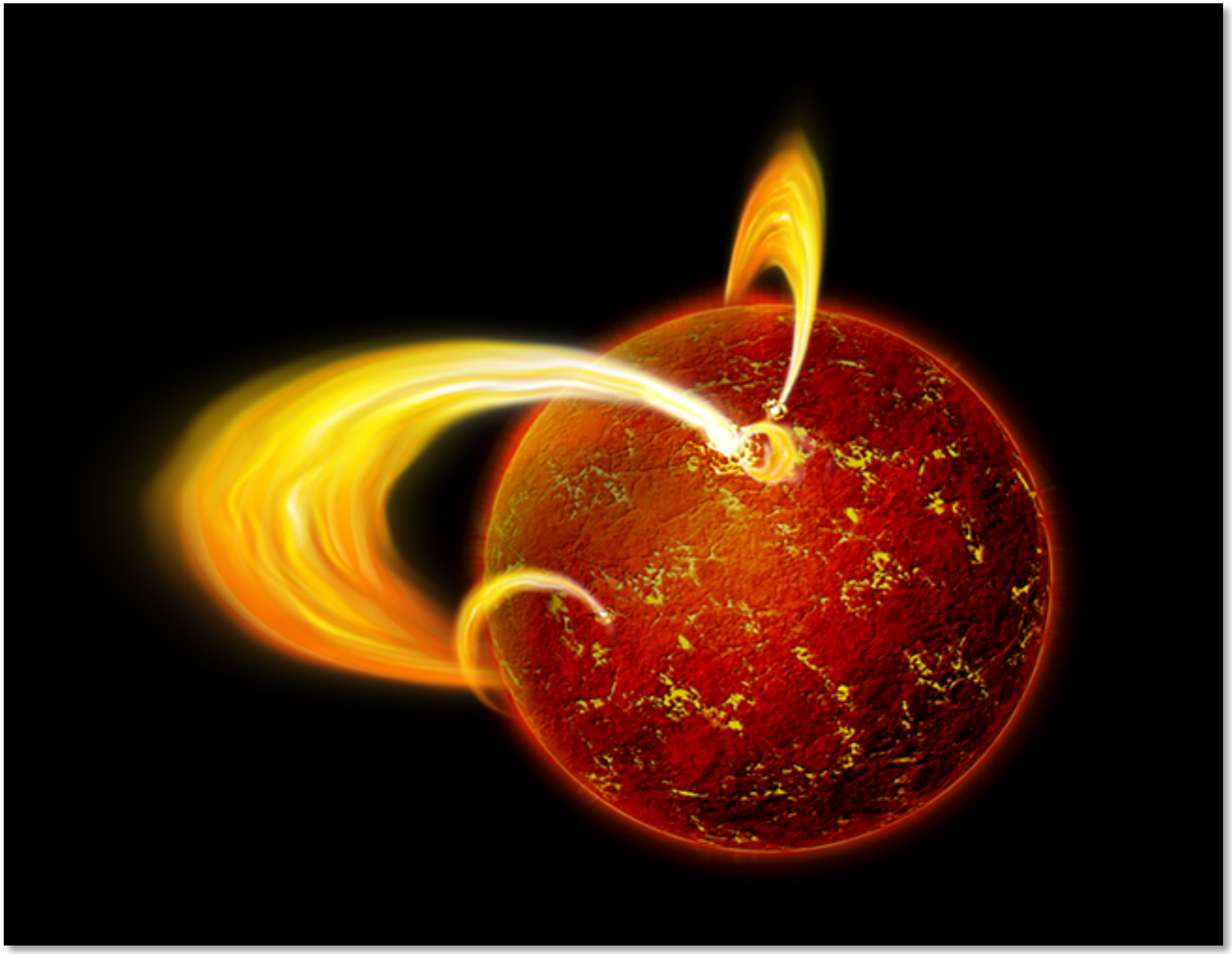

Magnetar Giant Flares

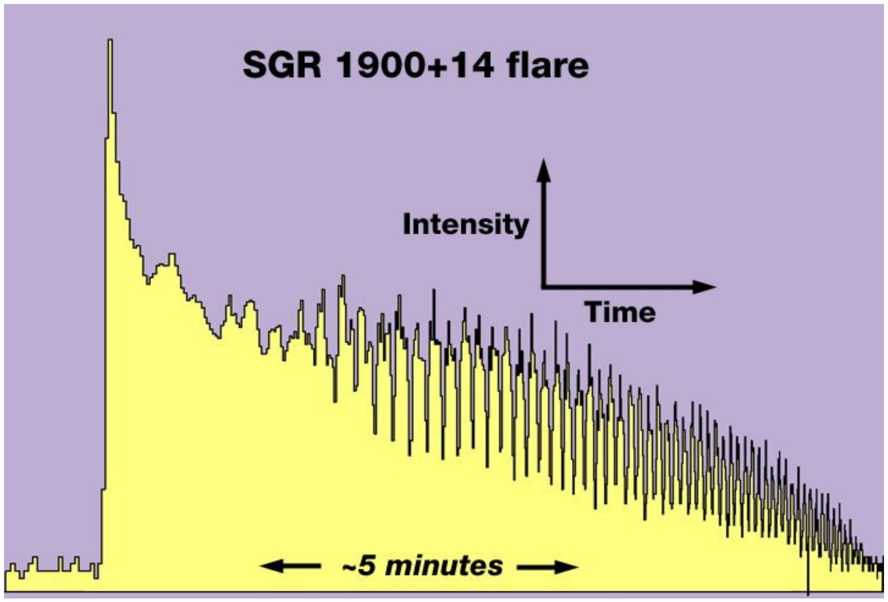

Three events to date:

- March 5th 1979: SGR 0526-66
- August 27th 1998: SGR 1900+14
- December 27 2004: SGR 1806-20

Powered by global magnetic instability (reconfiguration), crust fracturing.

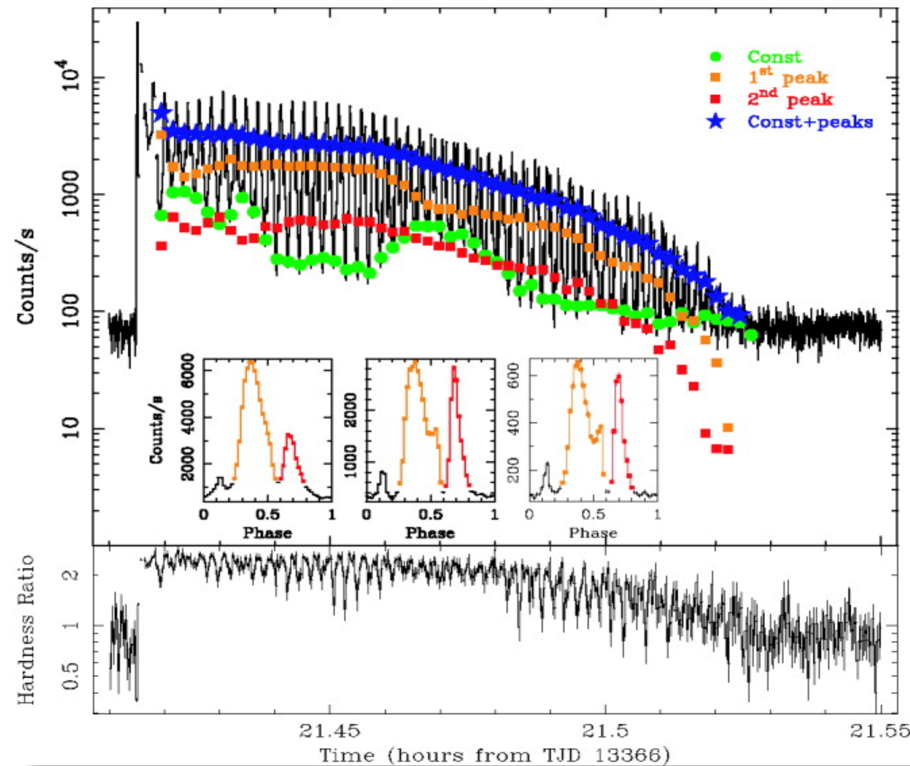

- Short, hard, luminous initial pulse.
- Softer X-ray tail persists for minutes, and reveals neutron star spin period.
- Emission from a magnetically confined plasma.
- 10^{15} G magnetic fields implied (TD 95)

Oscillations in the SGR 1806-20 Flare

- RXTE recorded the intense flux through detector shielding.
- Israel et al. (2005) reported a 92 Hz quasi-periodic oscillation (QPO) during a portion of the flare.
- Oscillation is transient, or at least, the amplitude time dependent, associated with particular rotational phase, and increased unpulsed emission.
- Also evidence presented for lower frequency signals; 18 and ≅ 30 Hz.
- Suggested torsional vibrations of the neutron star crust.

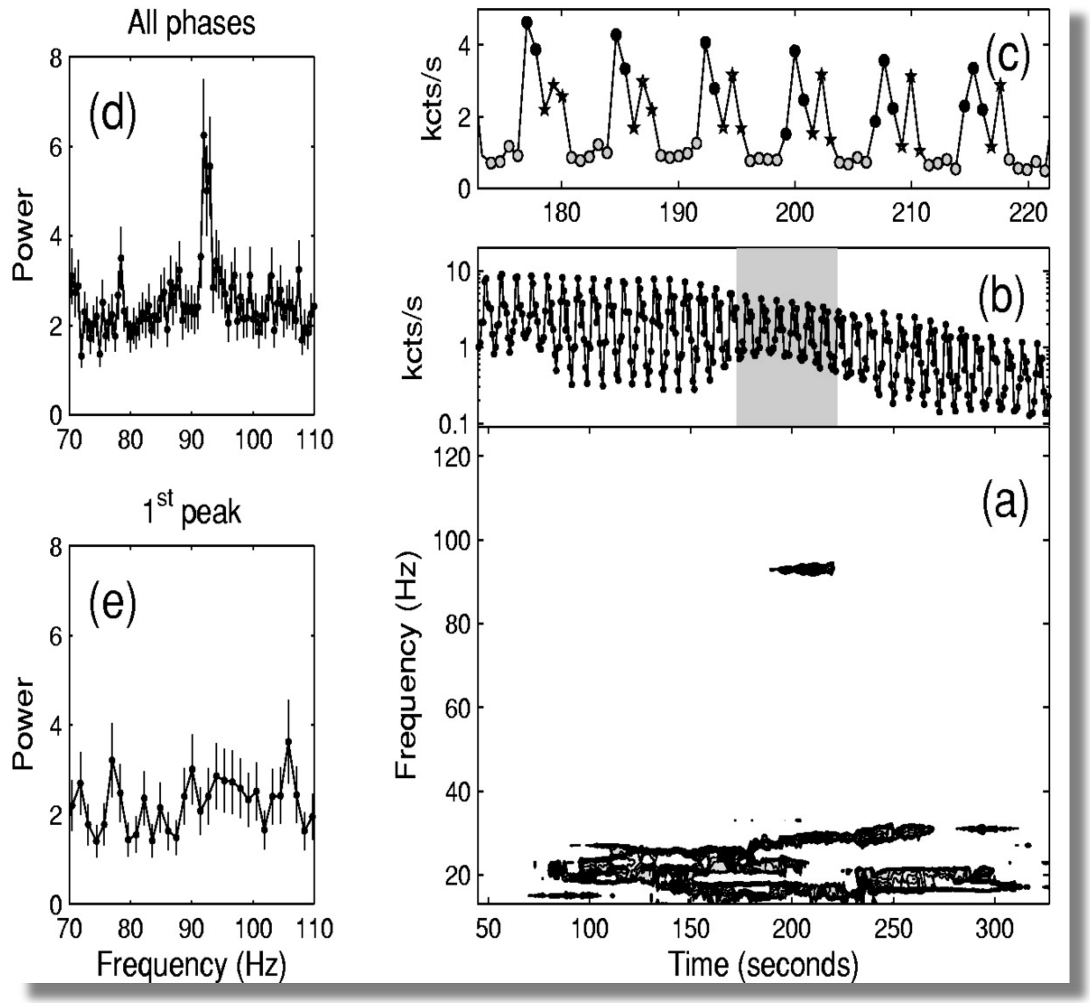

Israel et al. 2005

A Closer Look at SGR 1900+14

- SGR 1900+14 flare was observed in a manner very similar to the SGR 1806 flare.
- Same time resolution, but non-optimal read-out time resulted in data gaps.
- Initially searched each good data interval as a whole.
- 84 Hz QPO detected in 4th data interval searched. The first after the pulse structure had re-emerged.
- Strohmayer & Watts (2005)

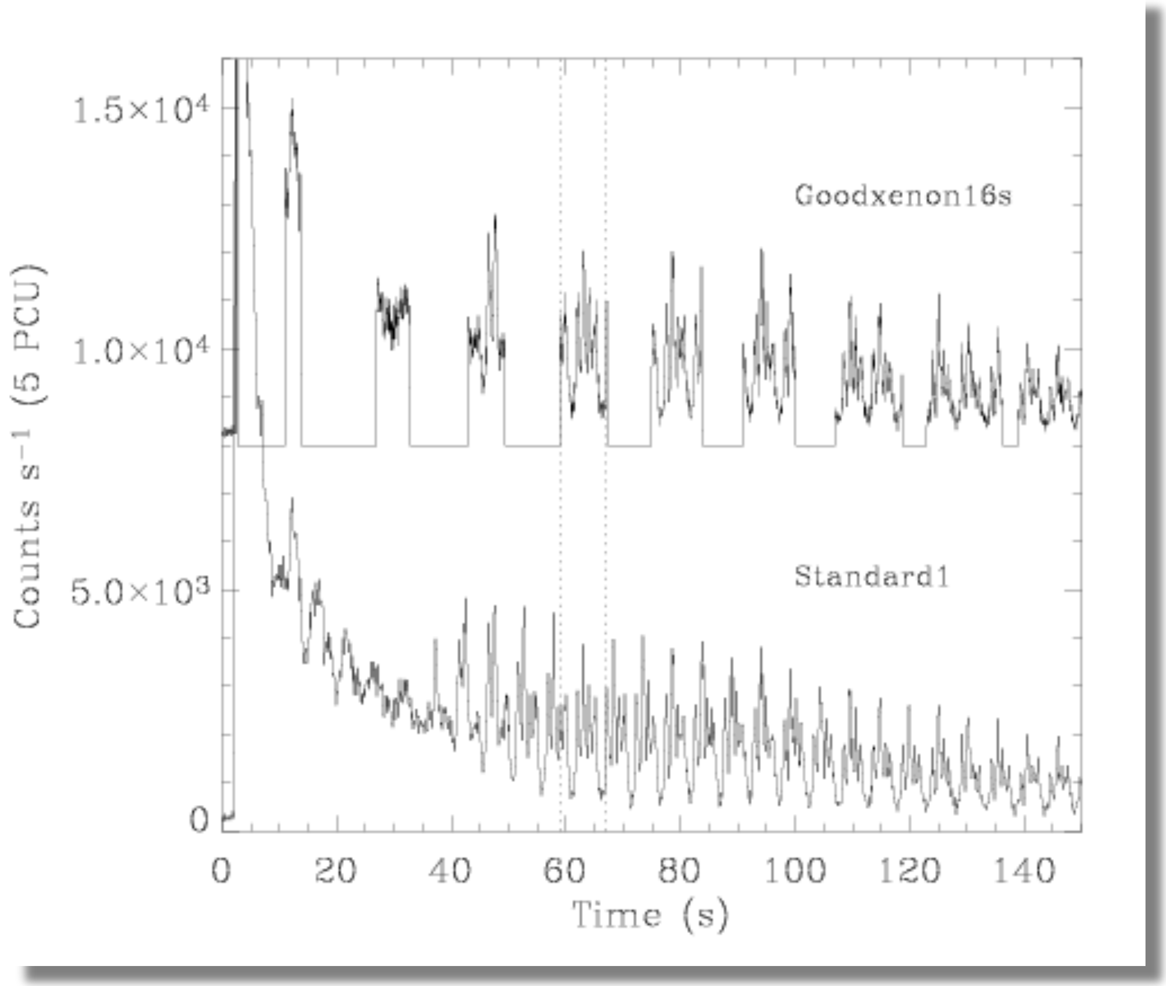

SGR 1900+14: 84 Hz signal

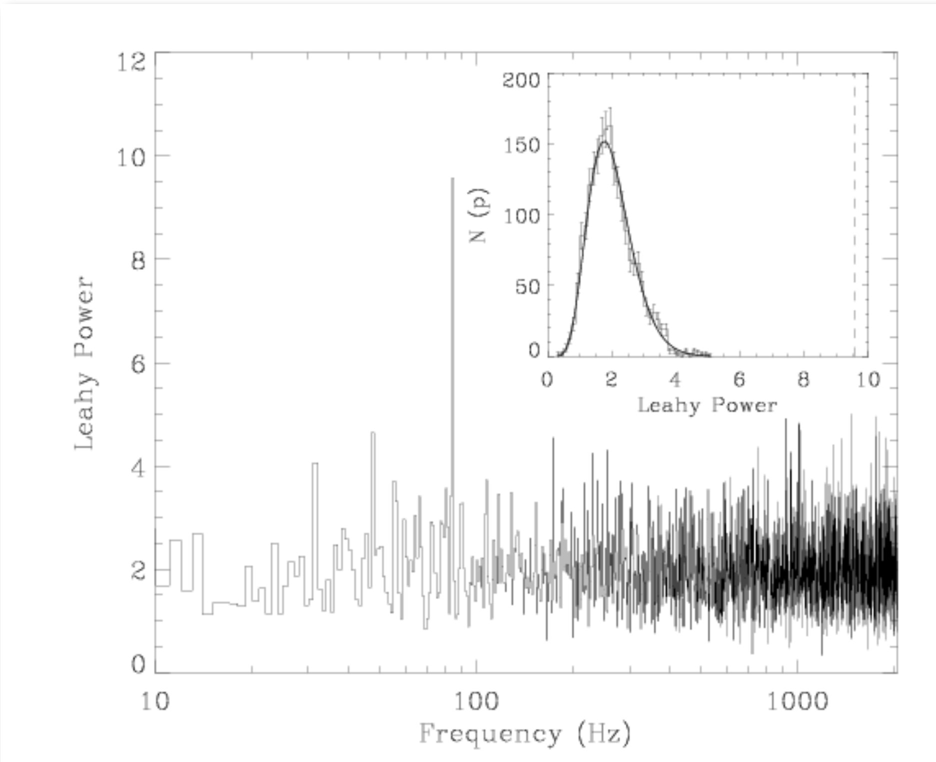

- 84 Hz signal localized in time (rotational phase).
- ~20 % (rms) amplitude
- Not centered on a pulse peak.

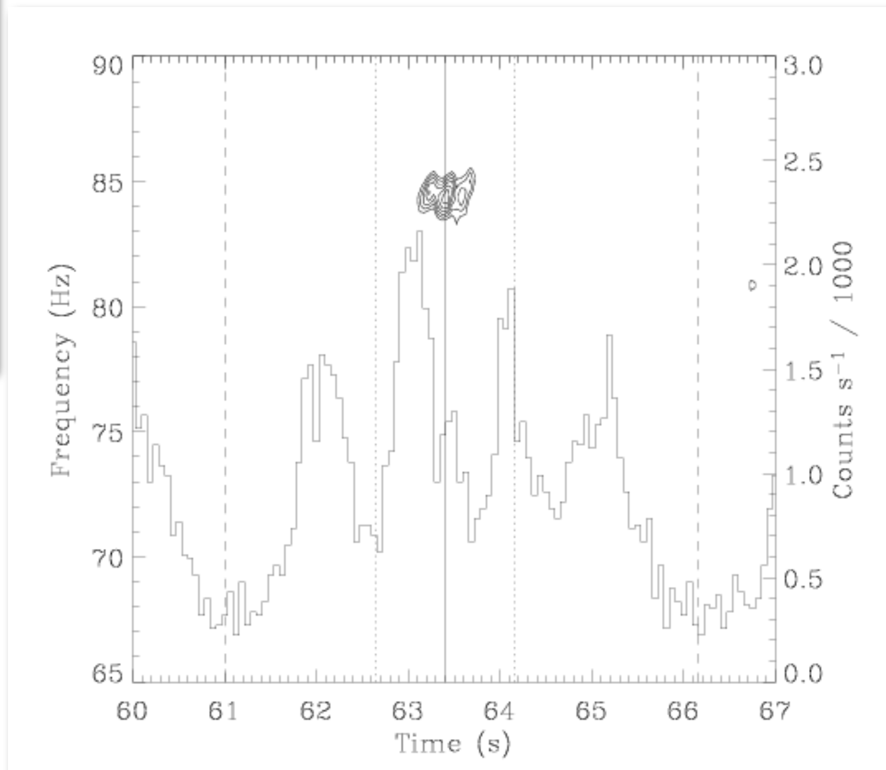

No other impulsive signals found, but what about weaker, persistent modulations?

SGR 1900+14: Other QPO Signals

- Computed average power spectra centered on the rotational phase of the 84 Hz QPO.
- A sequence of frequencies was detected: 28, 53.5, and 155 Hz!
- Amplitudes in the 7 – 11% range.
- Strong phase dependence: no signals detected from phases adjacent phase regions.
- 4 frequencies in SGR 1900+14, a sequence of toroidal modes?

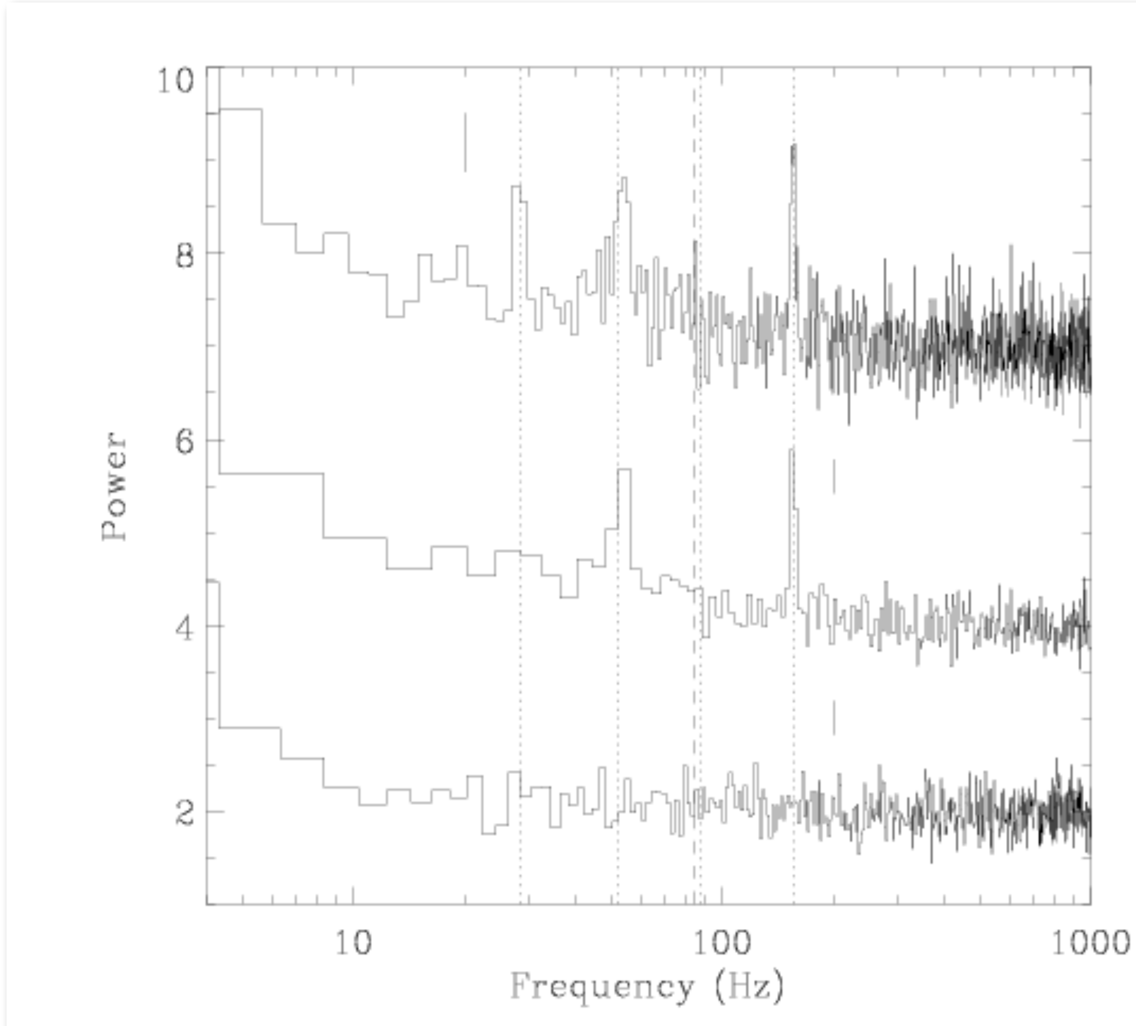

Persistence of QPOs: 1806-20

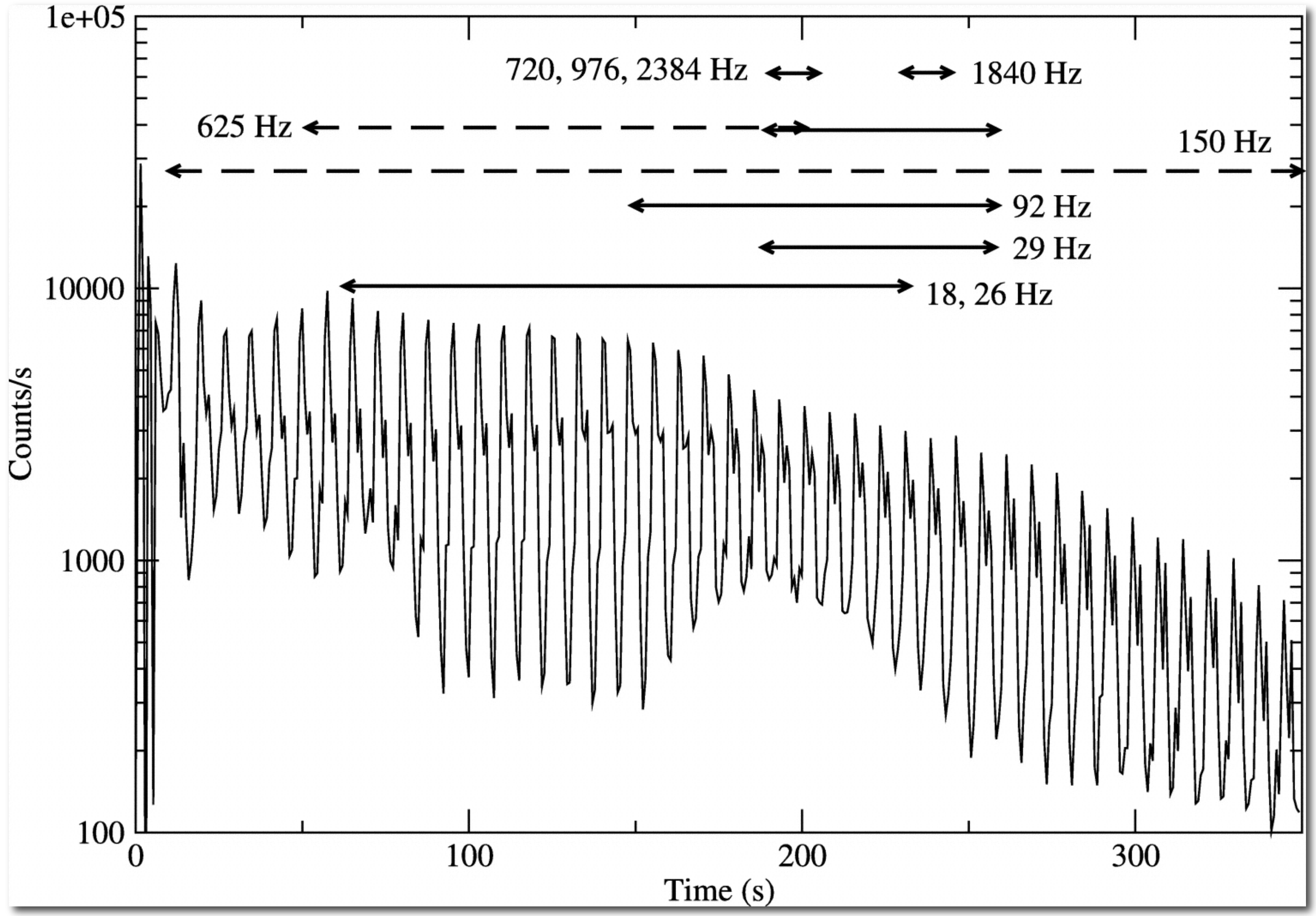

Time and Frequency Variations

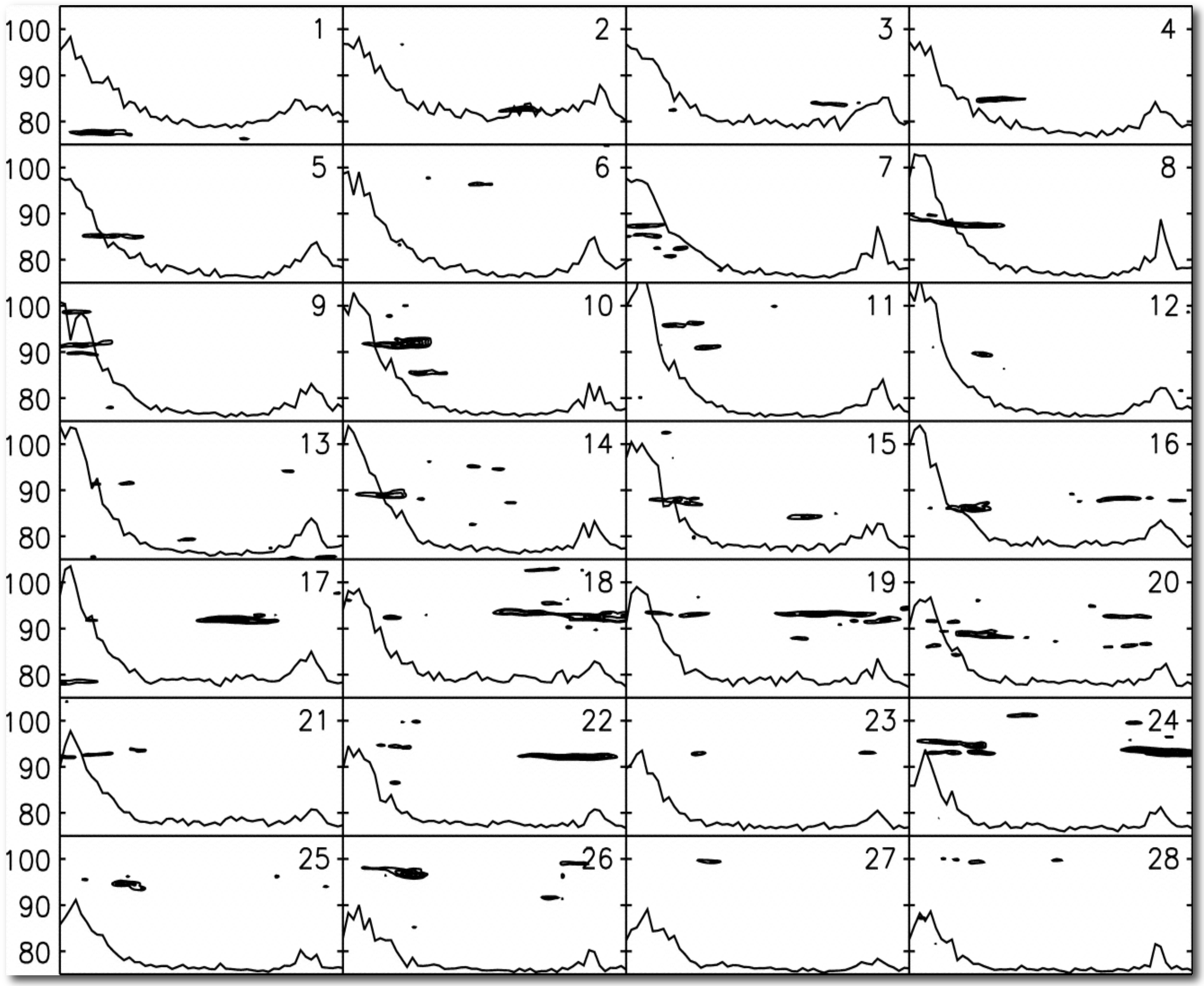

Strohmayer & Watts 2006

- 90 Hz QPO shows rather complex temporal, phase, and frequency variations.
- Amplitudes not constant in time (episodic).
- Several factors could be at work; changes in field and particle distributions. Energy exchange with the core.

Neutron Star Crusts: A Brief History

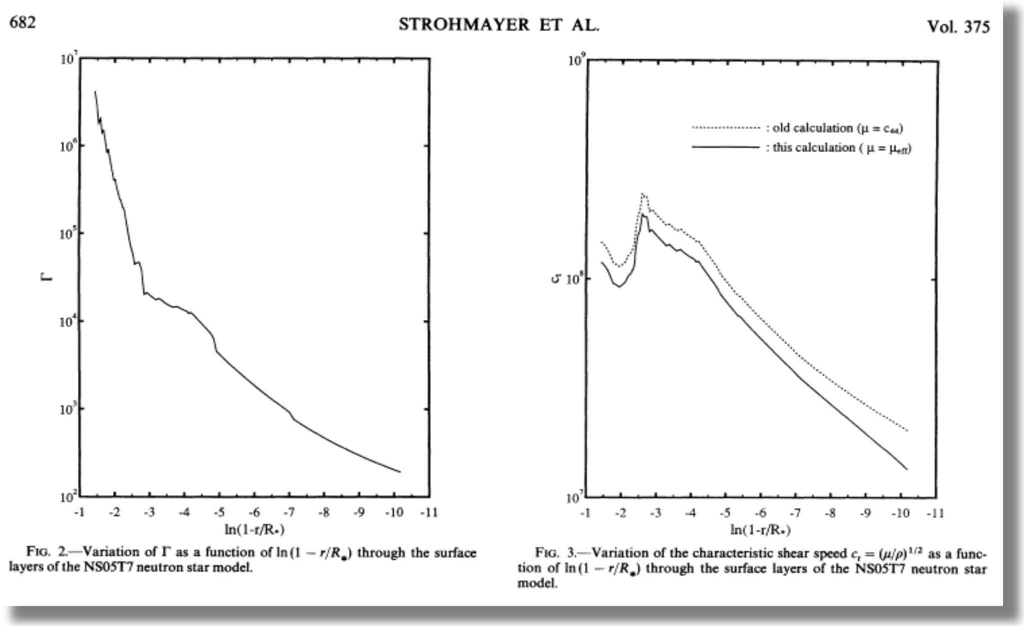

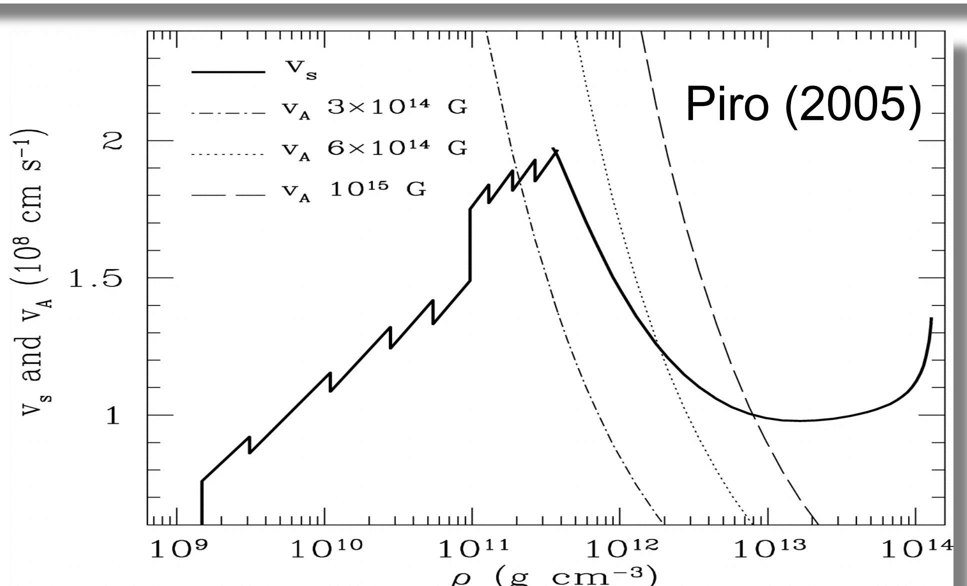

- Existence of a crust in a “normal” neutron star is not “controversial.” Ruderman (1968) suggested that radio pulsations from the first pulsars were due to torsional vibrations of crust.
- To good approximation crust is a Coulomb solid, that solidifies at $\Gamma = (Ze)^2 / akT > 175$.
- Ogata & Ichimaru (1990), Strohmayer et al. (1991) calculated μ and explored oscillation mode implications.
- Crust properties also linked with other observables, ie. Glitches and spin-down of pulsars, for example.

SGR 1900+14: Toroidal (torsional) Oscillation Modes

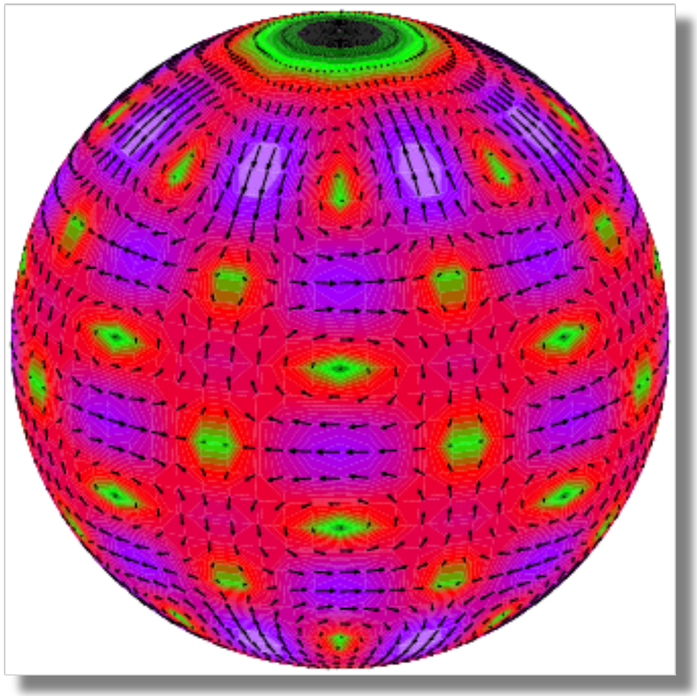

An l=7, m=4 toroidal mode (Anna Watts)

- A neutron star crust supports shear (toroidal) modes. Purely transverse motions. Modes studied theoretically (McDermott, Van Horn & Hansen (1988), Schumaker & Thorne (1983), Duncan (1998), Strohmayer et al. (1991).
- Angular dependence of modes described by spherical harmonic functions (*l, m*); and a radial eigenfunction (*n*), ${}_{l}t_{n}$
- *l* gives the total number of nodal planes, and *m* the number of azimuthal planes.

$$\nu({}_2t_0) = 29.8\,(R_{10})^{-1}\;(1.71 - 0.71M_{1.4}/R_{10})^{1/2}\;(0.87 - 0.13M_{1.4}/R_{10}^2)\ \mathrm{Hz}$$

$$\nu({}_lt_0) = \nu({}_2t_0)\,[\,l(l+1)/6\,]^{1/2}\;[1 + (B/B_\mu)^2\,]^{-1/2}$$

The SGR 1806-20 Flare: thickness of the crust

Strohmayer & Watts (2006)

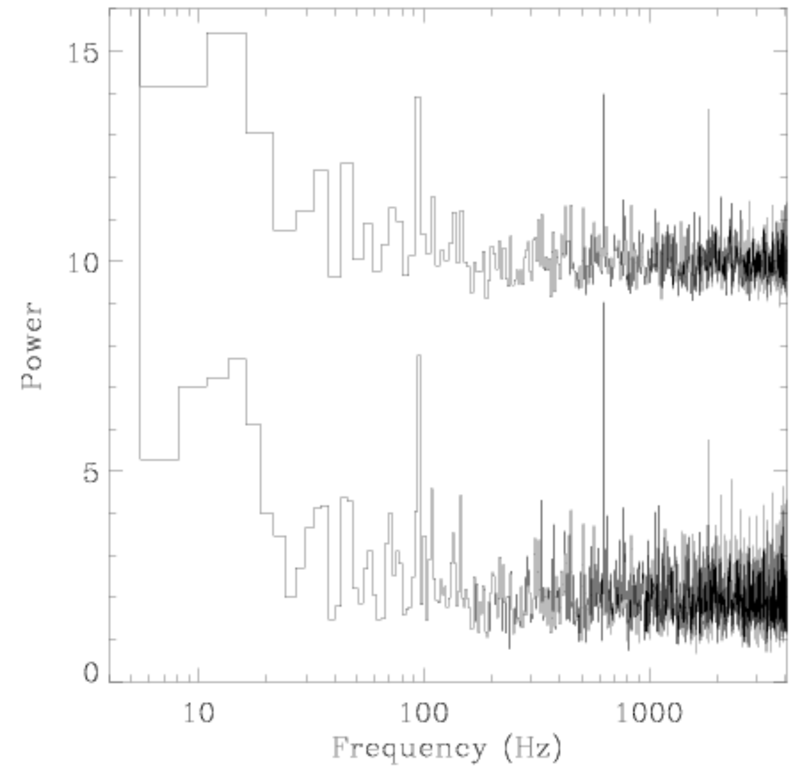

- For n = 0 modes, effective wavelength is R, for n > 0 it is ΔR, if V_s = constant, then $f_{n=0} / f_{n>0} \sim \Delta R/R$.

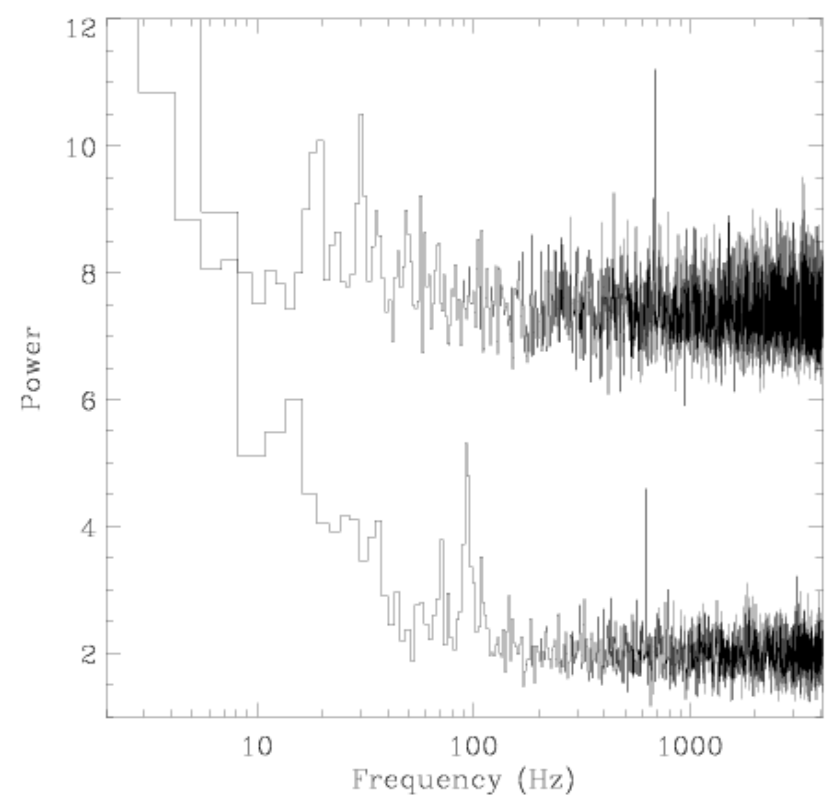

- Frequencies at 625 Hz and higher are likely n > 0 modes. Detection of n = 0 and n = 1 constrains crust thickness!

Implications for Neutron Star Structure

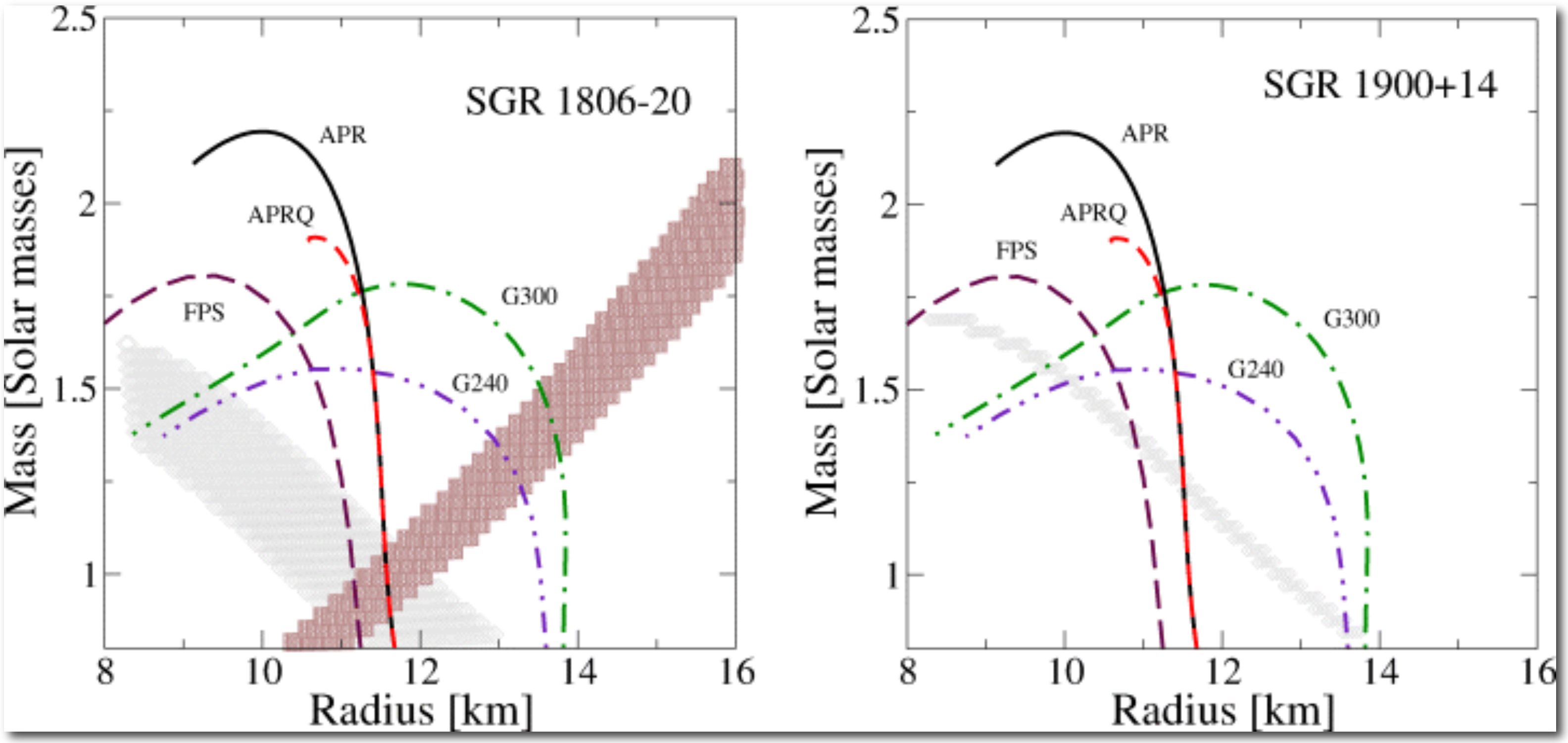

- Samuelsson & Andersson (2007) computed torsional modes in full GR (Cowling approximation).
- Determine "allowed" regions in M - R plane that can match observe mode sequences in SGRs 1806-20 and 1900+14.
- Caveat: No magnetic field corrections.

Crust - Core coupling

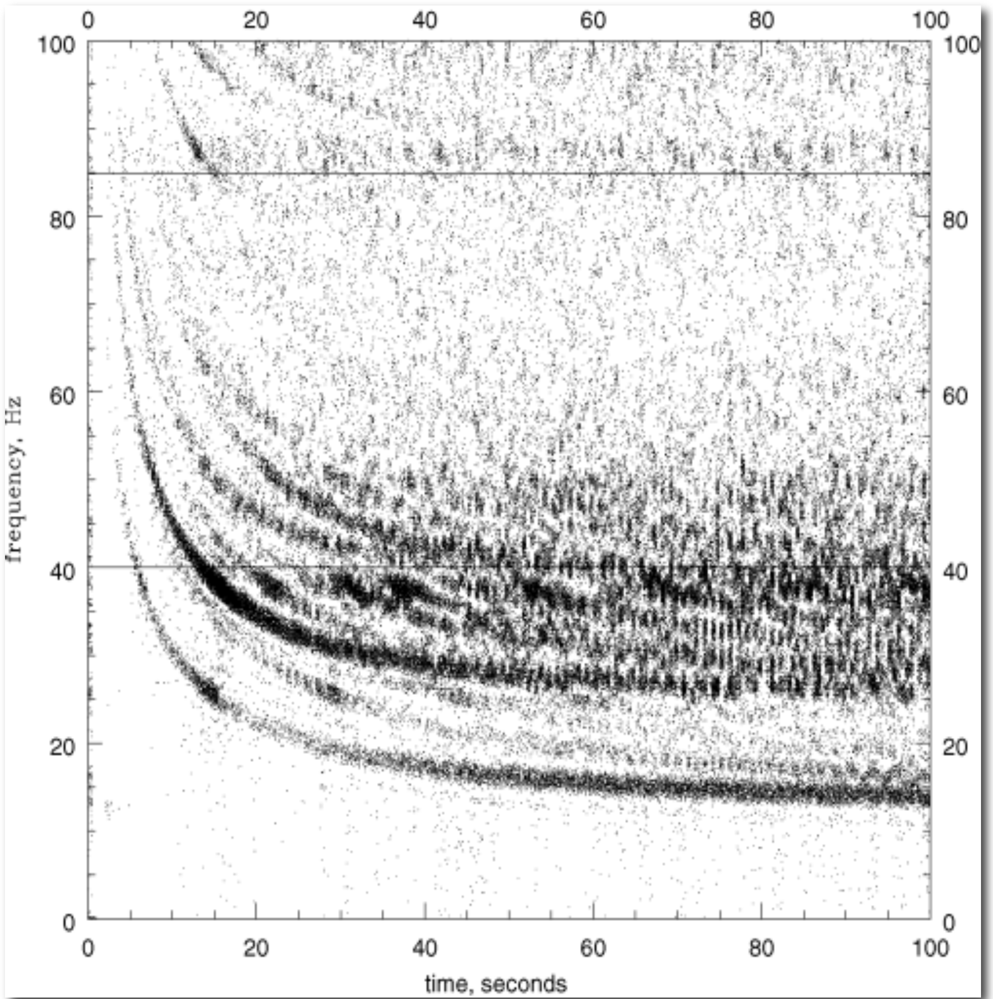

Levin (2007)

Levin argues that energy exchanges between the crust and a continuum of MHD modes in the core.

Solving initial value problem, finds QPOs excited at the so called “turning points” or edges of the MHD continuum. Lowest frequency modes (18, 25 Hz).

Also finds drifting QPOs, and amplification of these features near pure crust mode frequencies.

X-ray Modulation Mechanism

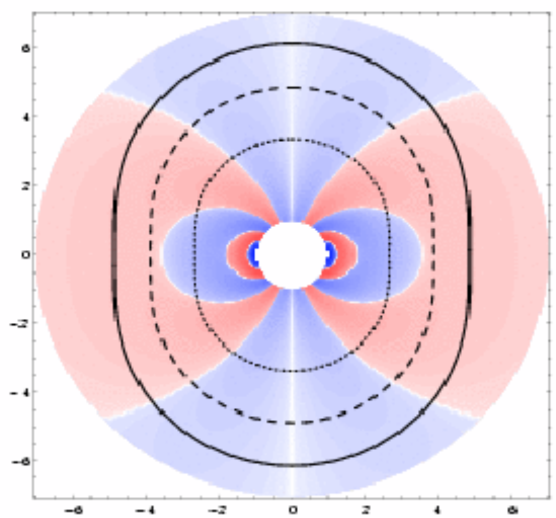

FIG. 1.— Current density distribution in the magnetosphere of a NS with dipole magnetic field oscillating in toroidal mode ($l = 10, m = 0$). The intensity of color in each point is proportional to $|j(r,\theta)|^{1/6}$ (this moderates contrast of the plot). Positive values of the current density are shown by red colors, negative ones by the blue color. By the black lines the resonant surfaces are shown for three photon energies $E_{ph} = 5; 10; 30$ keV – solid, dashed and dotted lines correspondingly. The magnetic field at the pole is assumed to be $B_0 = 10^{14}$ G.

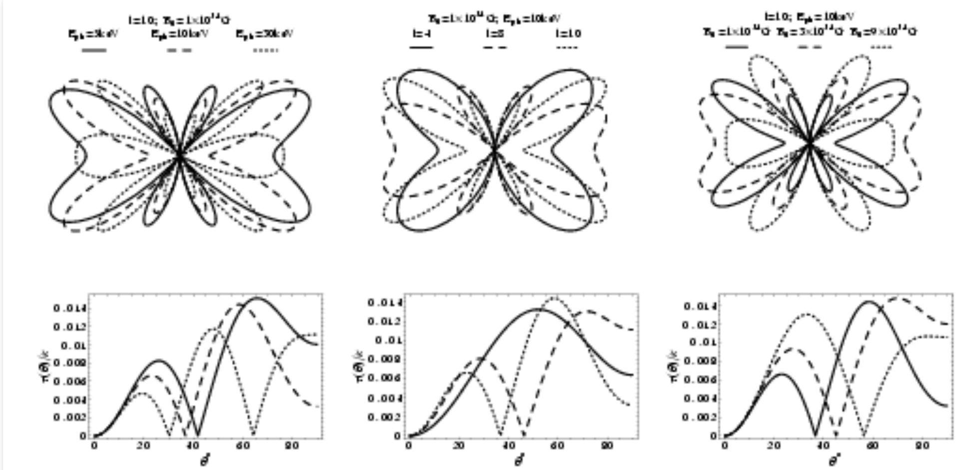

FIG. 2.— Angular distribution of the optical depths to resonant Compton scattering for radially moving photons in the magnetosphere of an oscillating NS for oscillations with the amplitude $\xi_0 = 0.01 R_{NS}$. In the upper figures the angular distribution $\tau(\theta)/\kappa$ is shown in polar coordinates $(\tau(\theta)/\kappa, \theta)$, in lower figures the same distribution is shown as a plot $\tau(\theta)$ for $\theta \in [0, 90^\circ]$. In the left figures the optical depth is shown for 3 different initial energies of the scattered photons ($E_{ph} = 5; 10; 30$ keV), the magnetic field $B_0 = 10^{14}$ G and the harmonic number of the toroidal mode $l = 10$ are fixed. In the middle figures the optical depth is shown for 3 different modes ($l = 4; 6; 10$), the magnetic field $B_0 = 10^{14}$ G and the initial energy of the scattered photons $E_{ph} = 10$ keV are fixed. In the right figures the optical depth is shown for 3 different values of the NS magnetic field ($B_0 = 1; 3; 9 \times 10^{14}$ G), the harmonic number of the toroidal mode $l = 10$ and the initial energy of the scattered photons $E_{ph} = 10$ keV are fixed.

Timokhin, Eichler & Lyubarsky (astro-ph/07063698)

Suggest that modulation of the particle number density in the magnetosphere by torsional motion of the crust produces the oscillations.

Estimate that 1% amplitude of crust motion needed to explain the observed QPO amplitudes.

The angular dependence of the optical depth to resonant Compton scattering may account for phase dependence.

Theoretical Issues

- Recognized that magnetic coupling of crust with core will likely be significant. Need "global" mode calculations (Levin 2006; Glampedakis et al. 2006; Sotani et al. 2006).
- Levin (2006) initially argued that torsional modes will radiate Alfven waves into the core and damp too quickly to be observed (~ 1 sec).
- Feedback, energy exchange between crust and core (Levin 2007).
- Excitation of modes in the crust, analogies with earthquake fractures.
- We see modulations in the X-ray flux, can these be produced by crust motions.
- Signal amplification, perhaps modest amplitudes are visible (beaming?)

Future Prospects, Missions in Planning

ASTROSAT (India)

Multiwavelength mission with several co-aligned instruments, including a PCA-like instrument.

PI: Prahlad Agrawal (TIFR)

Scheduled for launch in late 2012 (launch date has slipped several times)

- **LAXPC:** Collimated 3-80 keV proportional counter array with high-pressure gas, ~RXTE area
- **Sky monitor:** Very similar to RXTE ASM
- **Other instruments:** Soft X-ray telescope with 0.3-8 keV CCD; Coded-mask 10-150 keV hard X-ray imager; UV imaging telescope

Mission planning and scheduling not necessarily optimized for X-ray timing of transients and TOOs.

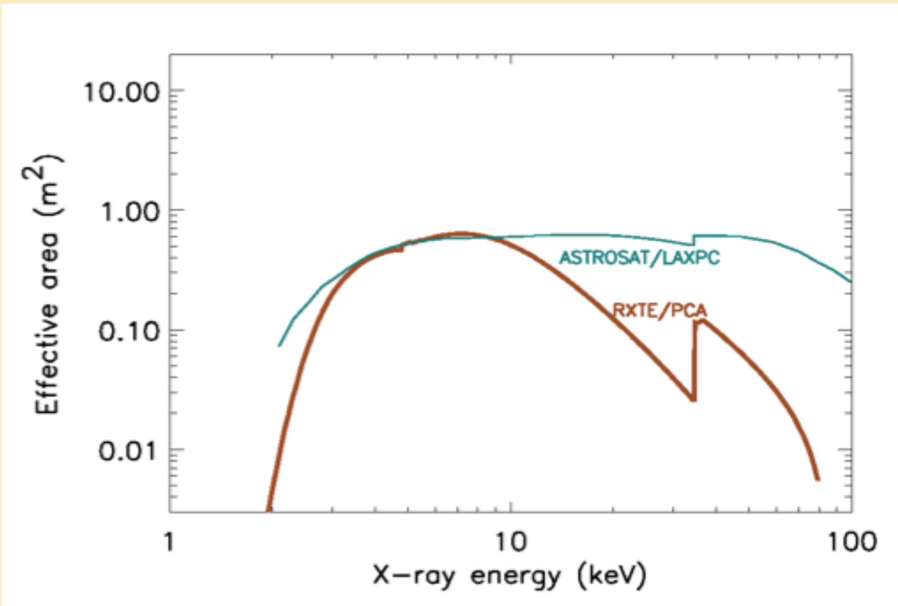

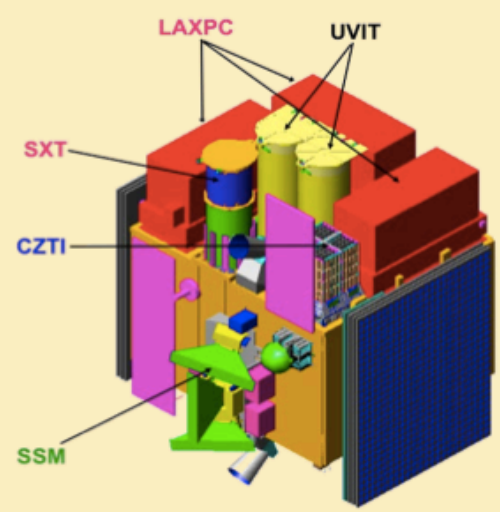

NICER: Neutron Star Interior Composition Explorer
(see poster 249.05 by Arzoumanian et al.)

0.2-12 keV soft X-ray timing and spectroscopy with concentrating optics, 2x XMM-pn area

Explorer MoO for International Space Station, selected by NASA for Phase A study in 2011. Downselect in 2013, launch in 2016.

PI: Keith Gendreau, Co-PI: Zaven Arzoumanian (NASA/GSFC)

- **Optics:** 56 grazing-incidence concentrators
- **Detectors:** 56 Si-drift detectors

Optimized for soft X-ray timing of thermal emission from isolated neutron stars

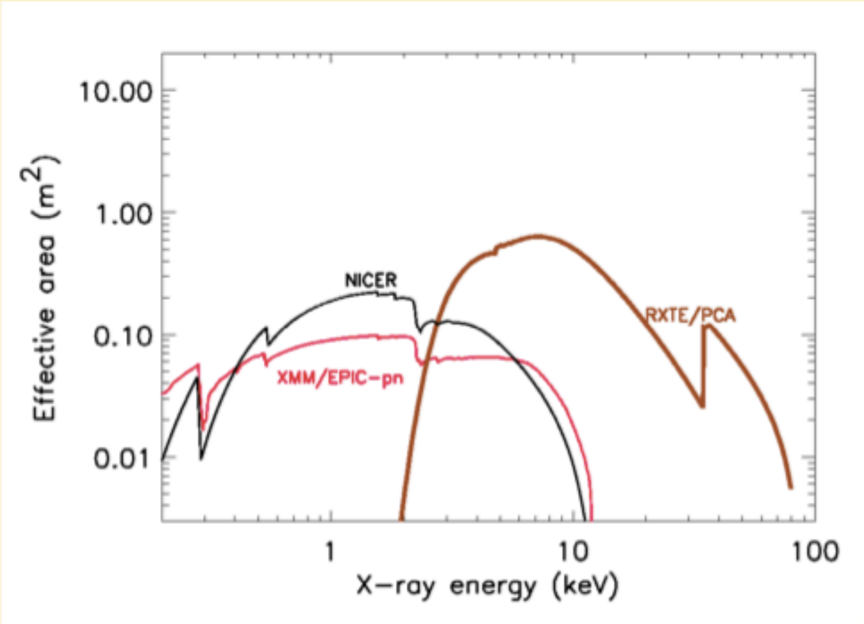

LOFT: Large Observatory for X-ray Timing
(see poster 249.06 by Ray et al.)

Collimated 2-50 keV X-ray timing and spectroscopy with ~20x RXTE

M (Medium) class mission selected by ESA for Assessment Phase in 2011. Downselect in 2013, launch in 2022.

• **Large-Area Detectors:** 10 m^2 area, ~250 eV resolution, Si-drift detectors, ultralight MCP collimators

• **Wide-field monitor:** 4 units, 2 coded-mask cameras each, 180°x90° FOV for entire WFM

U.S. participating in mission study and science working groups.

Issues: sky accessibility, response to transients